arXiv:1406.7521v4 [physics.atom-ph] 24 Apr 2015

Current progress in laser cooling of antihydrogen

E. V. Luschevskaya[1,*] and A. A. Golubev[2,1,†]

[1] National research centre "Kurchatov Institute" Institute of Theoretical and Experimental Physics, Bolshaya Cheremushkinskaya 25, Moscow, 117218, Russia

[2] National Research Nuclear University, Kashirskoye shosse 31, Moscow, 115409, Russia

We discuss laser cooling methods of (anti)hydrogen and its importance for current and future experiments. The exploration of antimatter presents a great interest for $CERN$ and GSI experiments aimed at check of quantum mechanics laws, fundamental symmetries of nature and gravity and investigations in atomic and nuclear physics. The spectral transition $1S \to 2P$ in $\bar{H}(H)$ atom is the most suitable for laser cooling due to a small lifetime of $2P$ state and insignificant ionization losses. However the pulsed and continuous laser sources at Lyman-α wavelength do not possess enough power for fast and efficient cooling. The small power of laser sources at $\lambda = 121.6$ nm is poor technical problem associated with a complexity of generation scheme of such radiation, which arises due to absence of nonlinear BBO crystals at this wavelength. The advances in this area will completely destine the future progress of the experiments aimed at study of antimatter.

1. INTRODUCTION

In 1931 Paul Dirac predicted the existence of positron [1, 2], which was discovered in cosmic rays by Karl Anderson two years later [3, 4]. In 1955 antiproton was found on the accelerator at the University of California.

In accordance with the CPT theorem any Lorentz invariant local quantum field theory with hermitian Hamiltonian must obey the CPT symmetry [5]. In other words there is antiparticle for every particle with the same mass, spin and lifetime, but with the opposite charge and magnetic moment. Violations of this theorem would imply new physical properties of fields and their interactions.

Antiparticles can be combined into antiatoms and antimolecules. An antihydrogen atom $\bar{H}$, the bound state of antiproton and positron, represents the simplest element of antimatter. In 1995 at $CERN$ antiproton ring $LEAR$ the first evidence of the antihydrogen existence was obtained. Nine antiatoms were detected, which moved with relativistic energies. It was impossible to make physical measurements because the observation period of antiatoms was very small [6].

In 1996 at Fermilab several dozens of antiatoms were found in a similar experiment [7]. It is worth noting that antihelium nuclei were detected at $IHEP$ in 1969 [8], much earlier than antihydrogen at $CERN$.

The construction of $CERN$ Antiproton Decelerator (AD) started in 1999 [9]. Currently this machine decelerates antiprotons down to energy ~ 5.3 MeV, it delivers $\sim 3 \times 10^7$ $\bar{p}$ per pulse ~ 150 ns, the duration of the cycle is 110 s. Then antiprotons move to various experiments. $ATRAP$ [10] and $ALPHA$ [11] experiments catch the antiprotons in a Malberg-Penning trap for further deceleration and cooling. $ASACUSA$ [12], ACE [13], $AE\bar{g}IS$ [14], $BASE$ [15, 16] experiments use a beam of antihydrogen atoms. $GBAR$ collaboration also plans to use a beam of antiatoms for further investigations [17]. The Extra Low ENergy Antiproton ring was proposed ($ELENA$) [18] to increase the number of accumulated antiprotons by one or two orders of magnitudes. $ELENA$ will become an upgrade of the Antiproton Decelerator. This new machine will supply $CERN$ experiments with antiprotons of 100 keV energy. So low energies could be achieved due to electron cooling [19].

For synthesis of antihydrogen atoms antiprotons are combined with positrons accumulated preliminarily in a positron trap [20–22]. $ALPHA$ collaboration obtains and detects antihydrogen since 2002 at $CERN$ [23], but at first they localized the antiatoms within the magnetic trap only in 2010 during 172 ms [24]. In 2011 confinement time of antihydrogen was approximately equal to 1000 s [25, 26]. In 2012 $ATRAP$ collaboration also synthesized the antihydrogen atoms in the magnetic trap [27].

At current experimental facilities antihydrogen formation occurs due to three-body recombination [28–31]

$$\bar{p} + e^+ + e^+ \to \bar{H} + e^+ \tag{1}$$

and recombination via resonant charge exchange [32, 33]

$$\bar{p} + Ps^* \to \bar{H}^* + e^+, \tag{2}$$

where Ps^* is the Rydberg positronium, the bound state of electron and positron in the excited state which can be produced via charge exchange collisions [34], $\bar{H}^*$ is the antihydrogen atom in an excited state. Theoretically $\bar{H}$ can be also produced via pulsed field recombination [35], radiative recombination (3) and laser-induced recombination (4) [29]

$$\bar{p} + e^+ \to \bar{H} + h\nu, \tag{3}$$

$$\bar{p} + Nh\nu \to \bar{H} + (N+1)h\nu. \tag{4}$$

$CERN$ collaborations synthesize antihydrogen for various goals, such as a search of distinctions between hydrogen and antihydrogen, gravitaional experiments, study of

*Electronic address: luschevskaya@itep.ru

†Electronic address: alexander.golubev@itep.ru

antiprotonic helium, measurement and comparison of the magnetic moments of proton and antiproton, antiproton therapy for cancer treatment and nuclear physics.

Theoretical studies show that violations of the CPT symmetry, if they exist, could be manifested in changes of frequencies of spectral transitions, Lamb shift and hyperfine structure of antihydrogen in comparison with hydrogen [36–38]. The deviations from the Standard Model can reveal itself in the violations of Lorentz and CPT symmetries. Antiatoms like any other antimatter can be a tool for testing of interaction dynamics of atoms and antiatoms [39]. The theoretical review about cold antihydrogen can be found in [40].

Collaboration $FLAIR$ (Facility for Low-energy Antiproton and Ion Research) in GSI research center in Darmstaadt also plans the study of antimatter and antihydrogen physics at their experimental facility. Their proposal is presented in [41]. It is supposed to improve the accuracy of precision experiments carried out at $CERN$ owing to a special antiproton slowing-down system. The main part of $FLAIR$ research aimed at study of antimatter and its interaction with matter and in particular with heavy nuclei.

The exploration of antimatter is an exciting scientific topic and undoubtedly deserve a large attention. W. Heisenberg in 1972 said: "I think that the discovery of antimatter was perhaps the biggest jump in physics in our century" [42].

2. HISTORY OF LASER COOLING

In 1975 T. Hansch and A. Schawlow [43] and independently D. Wineland and H. Dehmelt [44] proposed a new cooling method using laser irradiation based on Doppler effect. Later the first inspiring experiments were carried out with Mg^+ and Ba^+ ions held in a magnetic trap [45, 46]. This amazing action of light has many applications in science today. A large number of outstanding theoretical and experimental studies have been devoted to various schemes of laser cooling of neutral atoms, a reader can study the nobel papers [47–50], reviews [51–54] and books [55–57].

In 1976 V.S. Letokhov, V.G. Minogin and B.D. Pavlik proposed the chirp-cooling technique [58]. According to this method the frequency detuning of the cooling laser varies in time so that already chilled atoms stay in resonance with the light wave. This suggestion was successfully implemented in the experiment of D. Prodan and W. Phillips in 1983 [59, 60].

Later the theory of Doppler cooling was developed and improved significantly. The lowest temperature which could be achieved in this method was found for various conditions, for example in the presence of external magnetic field [61–67].

Zeeman cooling method was developed in 1982 by G. Metcalf [68]. Atoms moved from a high field region to a low field one as the atomic velocity decreased. So the shift of Zeeman sublevels compensates the decrease of Doppler shift and the laser frequency is maintained constant. Due to Zeeman cooling sodium atoms were slowed down to the velocity $\backsimeq 40$ m/s [69] and soon afterwards to 15 m/s corresponding to the temperature $\sim 100\,\mathrm{mK}$ [70]. The details of these experiments are also presented in [71–74]

In 1985 the group of scientists under the guidance of A. Migdal caught the sodium atoms in the quadrupole magnetic trap for one second [75], the trap depth was 17 mK which corresponds to the atomic velocity of 3.5 m/s.

In 1987 W. Phillips and his colleagues found disagreements between Doppler cooling theory and their experimental results. They studied the lifetime of optical molasses as a function of the laser frequency detuning. They got the minimal temperature $43\pm20\,\mu K$ much lower than the Doppler limit which is equal to 240 μK [53, 76].

J.Dalibard, C.Cohen-Tannoudji and S.Chu predicted and explained the observed effects from the theoretical point of view [77–79]. They showed that in a standing wave at low intensity of laser wave the subdoppler cooling might be provided either by spatial gradient of polarization or variable intensity. The minimal temperature was strongly dependent on the magnetic field value. So the subdoppler cooling was discovered. In 1997 J.Dalibard, C.Cohen-Tannoudji and S.Chu were awarded the Nobel Prize for their developments of cooling and trapping methods of atoms by laser field.

For the laser irradiation of high intensity the Sisyphus cooling scheme was suggested [80]. A strict correspondence between the theory and experiment hadn't been observed, but at the qualitative level the theory was confirmed by experimental results.

In 1990 the first evidences of optical lattices were obtained [81] and in the same year their first investigation had been carried out [82]. In 1990 W. Phillips with collegues cooled cesium atoms to 2.5 μK [83].

The next record temperature was achieved due to the method of adiabatic expansion, W. Phillips and his collegues reach the temperature 700 nK for sodium atoms [84]. However so low temperatures can be obtained only for the alkaline metals. The cases of helium and hydrogen are not so optimistic. There is some recoil temperature T_R determined by the relation $T_R = 2E_R/k_B$, where E_R is the recoil energy, k_B is the Boltzmann constant. For helium the recoil temperature is of the order of μK, for hydrogen atom it lies in the mK temperature range. This limit may be overcommed owing to the well known methods: velocity-selective coherent population trapping [85], Raman cooling [86] and sideband cooling for ions [44]. In all these technics the spontaneous irradiation processes are velocity dependent to prevent the light scattering by the coldest atoms.

In 1994 the velocity-selective coherent population trapping allows to get the temperature $T_R/2$ [87] for the beam of helium atoms and in 1997 the temperature $T_R/800$ for the precooled helium sample [88].

If we would have the laser sources required wavelength and power, these methods and their modifications may be applied for cooling of (anti)hydrogen. A laser cooling can be a preliminary procedure followed by evaporative cooling to get more dense and large condensates of atomic hydrogen. Cooling below one-photon recoil needs laser sources of very high power.

3. THEORY OF LASER COOLING

3.1. Radiation pressure

For the first time the assumption about interaction of light wave with a matter was made by J. Kepler in 17th century. He explained why tails of comets are elongated in the opposite direction from the Sun. In the 19th century Maxwell obtained the formula for the force of radiation pressure.

In 1901 P. Lebedev, E. Nichols and G. Hull in laboratory experiments proved that the light exerts pressure on various objects [89–91]. The experiment confirmed the theory despite a lack of a good vacuum. In 1910 P. Lebedev obtained more accurate results, which prove the Maxwell theory of light pressure [92].

Recoil phenomena arising due to reflection or scattering of the light induce radiation pressure forces which may be either resonant [93] or nonresonant. The nonresonant force acts on the atom or molecule when the frequency of the light wave is far from any resonant frequency of the particle. This force arises due to the Compton scattering of a photon.

V.S. Letokhov showed in [94] that the neutral atoms can be trapped by means of nonresonant forces. Namely for standing plane wave at intensities $\gtrsim 10^3 - 10^4$ W/cm^2 the atoms moving at small angles to the wavefront can be caught between nodes and antinodes of the standing wave owing to the dipole or striction force

$$f = \frac{1}{2} k_\omega \vec{\nabla}(\vec{E}^2). \tag{5}$$

$\vec{E}$ is the electric field strength, $k_\omega = (n_\omega - 1)/(2\pi N)$ is the atomic polarizability at the frequency ω of the external light field, n_ω is the refraction index of an atomic gas, N is the density of particles. So a configuration of standing waves in three mutually perpendicular spatial directions can serve the optical trap for atoms. However the number of particles moving at not large angles to the wavefront is small and the trapping requires significant costs of energy.

When the wave frequency is in resonance with an atomic spectral transition, the resonant force of light pressure appears, it may arise due to spontaneous or induced radiation [95].

In the case of spontaneous radiation the force arises due to the momentum recoil when the atom absorbs photons from an incident light wave. After the absorption of a light photon the excited atom emits another photon but in a random direction coming back to the ground state. An average contribution to the recoil force from the emission processes is zero because spontaneous irradiation can occur in any spatial direction.

The dipole force appears in the field of light standing wave during stimulated absorption and emission of photons by atoms along the direction of the incident wave.

In 1970 A. Ashkin studied the deflection of sodium atomic beam by light pressure forces [96] and obtained the formulas for scattering [97, 98] and dipole [98] forces acting on the atom in the field of a monochromatic light wave taking into account the saturation effect. V.S. Letokhov [99] and A. Ashkin showed that the scattering force alone is not sufficient to capture atoms [100], but it may accelerate [96, 101, 102] or slow down the atoms [43, 103].

Consider a two-level atom. It absorbs a photon with the momentum $\hbar\vec{k}$ and then reradiates another photon. The Doppler shift $\triangle\nu = p/(m\lambda)$ is less than the natural linewidth $\gamma = 1/\tau$ and we can average over a large number of radiation and absorption processes. So the spontaneously irradiated photons do not contribute to the average scattering force.

The resonant force acting on the atom in the optical molasses has the following form

$$\vec{F} = \frac{\hbar\vec{k}}{2\tau} \frac{I/I_0}{1 + I/I_0 + (2\delta\nu/\gamma)^2}\ , \tag{6}$$

where $\delta\nu = \nu - \nu_0 - \vec{k}\vec{v}/(2\pi)$ is the frequency detuning of the laser wave from resonance in the reference frame of the atom, ν is the frequency of the incident light, ν_0 corresponds to the resonant frequency of an atom moving with velocity $\vec{v}$, $k = 2\pi/\lambda$ is the wave vector. I is the intensity of the laser field, or energy flow density. I_0 is the saturation intensity

$$I_0 = \frac{4\pi^3\hbar c\gamma}{3\lambda^3}, \tag{7}$$

which corresponds to the irradiance when the level populations of the ground and excited states are equal.

Consider the case of two waves propagating in the opposite directions with the same frequency and intensity, the intensity of the waves is much less than the saturation intensity $I/I_0 \ll 1$. The total force is the sum of the scattering forces acting from the each wave and for $kv \ll \delta\nu$, $kv \ll \gamma$ has the following form

$$F = 4\hbar k \frac{I}{I_0} \frac{kv(2\delta)/\gamma}{[1 + (2\delta\nu/\gamma)^2]^2}. \tag{8}$$

When the laser frequency detuning is positive $\delta\nu > 0$, atoms accelerate and heat. For the negative frequency detuning $\delta\nu < 0$ the atoms slow down. The force considered here is equivalent to the viscous friction force $F = -\alpha v$ with the coefficient

$$\alpha = -4\hbar k^2 \frac{I}{I_0} \frac{(2\delta\nu)/\gamma}{[1+(2\delta\nu/\gamma)^2]^2}. \quad (9)$$

This analogy leads to the new conception of "optical molasses". Due to the absorption and emission of laser photons an atomic movement looks like the Brownian motion in a region restricted by laser beams [103]. The nonzero viscosity slows down the atoms in this region, however the optical molasses is not a trap and the viscosity force alone is not enough to capture neutral atoms.

3.2. Doppler cooling

An atom at rest equally absorbs light from both waves. At non-zero temperature the atom participates in the thermal motion. An atom moving with the velocity v sees the frequency of backward wave shifted to a higher frequency region by amount of Doppler shift $|\vec{k}\vec{v}|/(2\pi)$. We do not consider the second order Doppler effect here.

At $\delta\nu < 0$ an atom absorbs more photons from the counter-propagating wave than from the collinear one because the interaction cross section is larger for the backward wave. Spontaneous emission of light by an atom occurs in a random direction, and the average recoil force is zero. When the wave vector of a photon is opposite to the atom momentum, the atom losses energy and slows down [69]. This method of atoms deceleration is called the Doppler cooling [66, 104, 105].

The cooling process considered here competes with the phenomenon of random walks, i.e. the diffusion of atoms in optical molasses. At first the conception of optical molasses was introduced in [103] because an atom in the laser field moves like a particle in a viscous medium.

When the atom emits a photon randomly in an arbitrary direction it receives the recoil momentum $\hbar k$. The average atomic momentum $\langle\vec{p}\rangle$ doesn't vary, but its mean square $\langle(\vec{p})^2\rangle$ changes for the value of $\hbar^2k^2$ after an each photon emission. This results to an increase of the average kinetic energy of the atoms, i.e. heating. There is a certain temperature limit of the Doppler cooling determined by the configuration of laser beams and magnetic fields in a cooled volume.

D.Wineland and V.Itano calculated in one-dimentional case [66] the Doppler limit when $|kv| \ll |\delta|$, $|kv| \ll \gamma$, $I/I_0 \ll 1$ both for the case of free atoms and atoms subjected to the external magnetic field. The cooling rate is determined by the decrease rate of the particle kinetic energy

$$\left(\frac{dE}{dt}\right)_{\text{cool}} = Fv = -\alpha v^2, \quad (10)$$

where the coefficient α is defined by (9).

The heating rate

$$\left(\frac{dE}{dt}\right)_{\text{heat}} = \frac{\hbar^2k^2}{M} \frac{\gamma I/I_0}{1+(2\delta\nu/\gamma)^2}, \quad (11)$$

where M is the mass of an atom. The minimal temperature of the Doppler cooling is determined by the equal rates of heating and cooling $(dE/dt)_{\text{heat}} = -(dE/dt)_{\text{cool}}$. Therefore taking into account the equality $m\langle v^2\rangle/2 = k_BT/2$ we get

$$T = \frac{\hbar\gamma^2}{8k_B|\delta\nu|}(1+(2\delta\nu/\gamma)^2), \quad (12)$$

where k_B is the Boltzman constant. The minimum temperature can be found from (12) keeping the frequency detuning equal to the half of the level width $\delta\nu = -\gamma/2$ during cooling, then the Doppler limit is equal to

$$T_{\text{dop}} = \hbar\gamma/(2k_B). \quad (13)$$

One can find the Doppler limit for three orthogonal laser beams [53], the cooling rate will be the same as in one-dimensional case however the heating rate will be in three times larger. Since $m\langle v^2\rangle_{3D}/2 = 3k_BT/2$ then we get the same Doppler limit (13) as in the one-dimensional case.

3.3. Role of dipole force

Consider a neutral atom in an external light wave. Electrons of the atom oscillate under the influence of an alternating electric field and irradiate electromagnetic energy. If the intensity of the light field is large enough then the atom radiates coherently with the external light field. Such radiation is called stimulated or induced. During radiation dipole or gradient force acts on the atom (5).

At small intensity of laser wave ($I/I_0 \ll 1$) the dipole force is much smaller than the scattering force and usually can be neglected. However at very small temperatures, when the Doppler cooling doesn't work anymore, the atoms can be cooled owing to the dipole force, which acts even on the atoms at rest. This is subdoppler cooling and we discuss its mechanisms in the next section.

Strong dipole force acts on the atom in a very intense light wave at $I/I_0 \gtrsim 1$. The fast laser cooling due to dipole force is possible in a standing wave created by two counterpropagating laser waves of high intensity. The atom can absorb the photon from one laser wave and reradiate it in another laser wave. Such interaction with the both plane waves leads to the appearance of dipole force.

Jan Dalibard in his PhD dissertation gave a precise expression for the damping coefficient α for an atom moving in a standing wave. This result was obtained with help of perturabative approach [106]. It is valid if $|kv| \ll \gamma$ and has the following form

$$\alpha = -\frac{\hbar k^2}{(1+4s)^{3/2}}\Big[\frac{4s(2\delta\nu/\gamma)}{1+(2\delta\nu/\gamma)^2}(1+2s) \quad (14)$$

$$-\frac{2\delta}{\gamma}[1+6s+6s^2-(1+4s)^{3/2}]\Big],$$

where $s = \frac{I/I_0}{1+(2\delta\nu/\gamma)^2}$ is the saturation parameter.

To eliminate the effects of simultaneous interaction with both plane waves one can consider two counter-propagating waves with different σ^+ and σ^- polarizations (relative to each other the polarization vectors will rotate in the same direction). The only transition allowed is $J = 0 \to J = 1$. The damping coefficient has the following form

$$\alpha = -\frac{2\hbar k^2 s}{1+2s}\frac{2(2\delta\nu/\gamma)}{(2\delta\nu/\gamma)^2 + [1+0.5s[(2\delta/\gamma)^2+1]]^2} \quad (15)$$

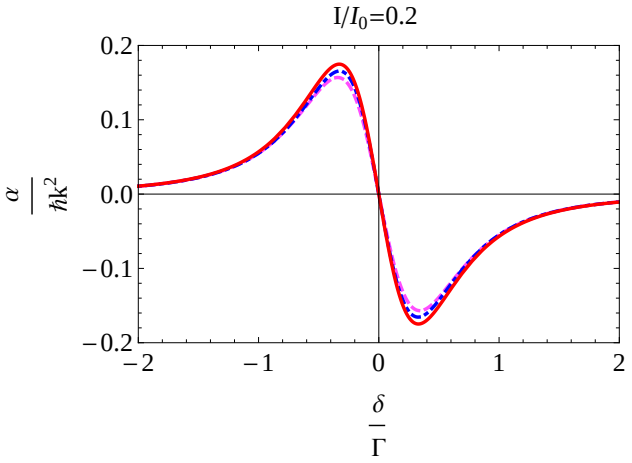

FIG. 1: Damping coefficient in units $\hbar k^2$ versus detuning of the laser wave for classical molasses (solid), standing wave (dashed-dotted), and $\sigma^+ - \sigma^-$ (dashed) for $I = 0.2I_0$.

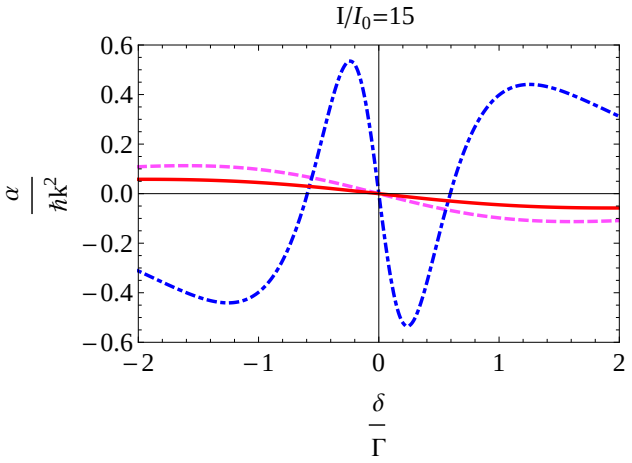

FIG. 2: The same that on Figure 1, but for $I = 15I_0$.

In Figures 1 and 2 we see the illustration to this behaviour. The damping coefficients $\alpha/(\hbar k^2)$ are shown versus the value of detuning.

The solid lines correspond to the one-dimensional classical molasses, the dashed-dotted lines represent the damping coefficient for a standing wave, the $\sigma^+ - \sigma^-$ wave configuration is depicted by the dashed lines.

At the intensity $I = 0.2I_0$ all three cases almost do not differ, because dipole forces are small. Red detuning $\delta\nu < 0$ provides cooling and slowing of atoms, blue detuning $\delta > 0$ leads to heating.

At the intensity $I = 15I_0$ the field of standing wave results in much faster cooling than classical molasses or the $\sigma^+ - \sigma^-$ wave configuration. In a standing wave at high intensity the atom subjected to a very strong damping force either for blue detuning at $\delta\nu \gtrsim 0.6\Gamma$ or for slightly red detuned laser wave.

Therefore dipole forces also can lead to the heating of neutral atoms at negative laser wave detuning. J.Dalibard and C.Cohen-Tannoudji explained this effect due to a concept of dressed states [79]. They suggested to consider an atom interacting with both counterpropagating waves. For comparison in the case of classical molasses at red detuning the atom interacts with counterpropagating running wave, at blue detuning with codirectional laser wave mainly, see previous Section.

3.4. Conception of dressed states

In the approach of "dressed states" the energy levels of combined atom-laser wave system are considered. This approach is valid if the coupling between atom and laser wave is large, i.e. the Rabi frequency $\omega_1 \gg \gamma$, where γ is the natural linewidth of the excited level and $\omega_1 = \vec{d}\cdot\vec{E}/\hbar$, $\vec{d}$ is the atomic electric-dipole moment. This theoretical model is in agreement with experimental results [107].

Consider a semiclassical approximation, when the size of the atomic wave packet is small compared with the laser wavelength $\triangle r \ll \lambda$ and $k\triangle v \ll \gamma$. The frequency detuning $\delta = \omega_L - \omega_0 \ll \omega_L, \omega_0$, where ω_L is the frequency of laser wave, ω_0 is resonance frequency of atomic transition. The quantum-mechanical Hamiltonian of atom-laser wave system in dressed state approach has the following form

$$H_{DA}(\vec{r}) = \hbar(\omega_L - \delta)b^+b + \hbar\omega_L a_L^+ a_L - \quad (16)$$

$$-[d\cdot\vec{\mathcal{E}}_L(r)b^+a_L + d\cdot\vec{\mathcal{E}}_L^*(r)ba_L^+].$$

The kinetic energy of the atom $\vec{P}^2/2m$ is not considered here. In (16) the first term corresponds to the internal atomic energy, the second term is the energy of radiation field, the third one expresses the interaction between atom and laser field. a^+ and a are the destruction and the creation operators of a photon, $b = |g\rangle\langle e|$ and $b^+ = |e\rangle\langle g|$ are lowering and raising operators,respectively, g denotes ground atomic state, e corresponds to the excited state.

In (16) $\vec{\mathcal{E}}_L(\vec{r})$ and $\vec{\mathcal{E}}_L^*(\vec{r})$ are defined through the positive and the negative frequency components of the electric field

$$\vec{E}^+(\vec{r}) = \vec{\mathcal{E}}_L(\vec{r})a_L, \quad \vec{E}^-(\vec{r}) = \vec{\mathcal{E}}_L^*(\vec{r})a_L^+. \quad (17)$$

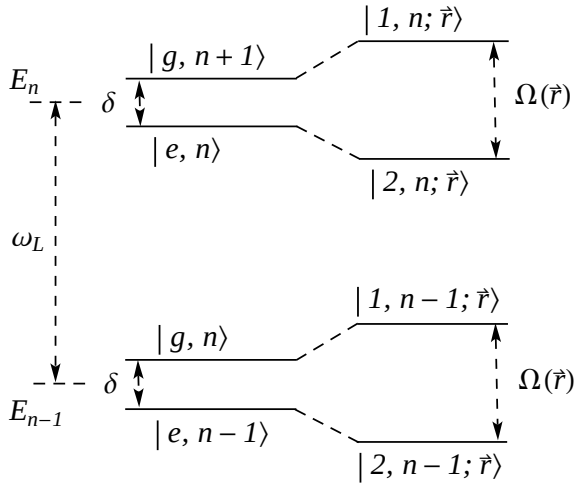

FIG. 3: Diagram of energy levels. In the left part of the figure the levels of atom-laser wave system is shown without interaction between laser field and atom. In the right part the dressed states are depicted depending on the atomic position $\vec{r}$ in space.

At high intensity the last term in (16) has to be taken into account, because it is responsible for the interaction of atomic levels with the electric field of laser wave. This interaction is defined by the matrix element

$$\frac{2}{\hbar}\langle e, n|V|g, n+1\rangle = -2\sqrt{n+1}\frac{d\mathcal{E}}{\hbar} = \tag{18}$$

$$= \omega_1(\vec{r})\exp[i\phi(\vec{r})],$$

where $\phi(\vec{r})$ is the relative phase between the vector of dipole moment d and the vector of external electric field $\vec{E}$.

Introduce the concept of generalized Rabi frequency

$$\Omega(\vec{r}) = [\omega_1^2(\vec{r}) + \delta^2]^{1/2}, \tag{19}$$

then the eigenstates of Hamiltonian of atom-standing wave system have the form

$$E_{1n}(\vec{r}) = (n+1)\hbar\omega_L - \frac{\hbar\delta}{2} + \frac{\hbar\Omega(\vec{r})}{2},$$

$$E_{2n}(\vec{r}) = (n+1)\hbar\omega_L - \frac{\hbar\delta}{2} - \frac{\hbar\Omega(\vec{r})}{2}. \tag{20}$$

and shown in Fig.3 schematically for zero and non-zero Rabi frequency.

For the case of small induced dipole moment (the intensity of laser field is small) the levels picture is presented in left part of Fig.3, there are two sets of states corresponding two atomic energy levels and not interacting with laser field of standing wave. The following notations are used: the difference between E_n and E_{n-1} is equal to the energy of one laser photon $\hbar\omega_L$. Each level has

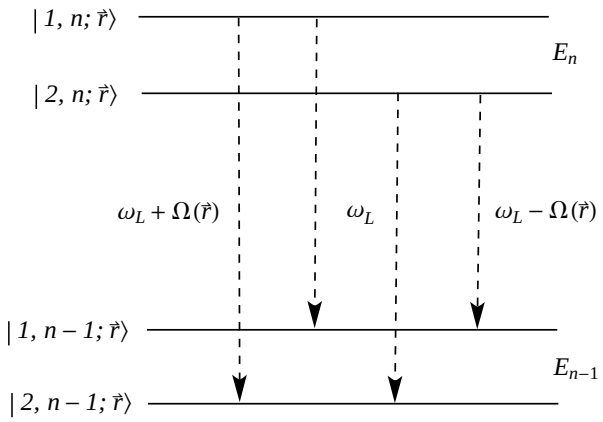

FIG. 4: Spontaneous transitions between various atomic energy states at some coordinate $\vec{r}$.

a pare of states: one ground and one excited state. For example the level E_n has one ground state $|g, n+1\rangle$ with the number of laser photons $n+1$ and one excited state $|e, n\rangle$ with the corresponding number of laser photons n.

For the case of non-zero Rabi frequency we obtain the picture in the right part of Fig.3, the states $|1, n; \vec{r}\rangle$ and $|2, n; \vec{r}\rangle$ at the position $\vec{r}$ of the atom. The eigenvectors of hamiltonian (16)

$$|1, n; \vec{r}\rangle = \exp[i\phi(\vec{r})/2]\cos\theta(\vec{r})|e, n\rangle$$

$$+ \exp[-i\phi(\vec{r})/2]\sin\theta(\vec{r})|g, n+1\rangle,$$

$$|2, n; \vec{r}\rangle = -\exp[i\phi(\vec{r})/2]\sin\theta(\vec{r})|e, n\rangle$$

$$+ \exp[-i\phi(\vec{r})/2]\cos\theta(\vec{r})|g, n+1\rangle, \tag{21}$$

where angle $\theta(\vec{r})$ is defined by the following expressions

$$\cos 2\theta(\vec{r}) = -\frac{\delta}{\Omega(\vec{r})}, \quad \sin 2\theta(\vec{r}) = \frac{\omega_1}{\Omega(\vec{r})}. \tag{22}$$

So the dressed states are the superposition of the ground and excited states in the field of electromagnetic wave (21). In the absence of laser field the distance between levels is equal to $\hbar\delta$ in energy units. Inside the intense laser beam the distance between levels is equal to $\hbar\Omega(\vec{r})$ and can be much larger than the value of $\hbar\delta$.

The value of energy gap between the ground and excited states depends on the atom position $\vec{r}$. Without interaction with intense electromagnetic laser wave there is only one transition in an atom: from $|e, n\rangle$ state to $|g, n\rangle$ state. If the atom interacts with the laser wave, three additional transitions appear.

The all transitions are shown in Fig.4 by dashed lines. Two transition occur at the same frequency ω_L, other two corresponds to the frequencies $\omega_L + \Omega(\vec{r})$ and $\omega_L - \Omega(\vec{r})$.

So called triplet Mollow was obtained in experiment and confirmed the theory [108]. Results of experiment [107] also agree with this theory.

The expression for gradient force acting on the atom at rest was obtained in [79]

$$f_{\rm dip}^{\rm rest} = -\nabla\left[\frac{\hbar\delta}{2}\log\left(1+\frac{\omega_1^2}{2\delta^2}\right)\right] \quad (23)$$

For atom moving with velocity $\vec{v}$ the dipole force

$$f_{\rm dip}(\vec{r},\vec{v}) = f_{\rm dip}^{\rm rest} - \frac{2\hbar\delta}{\Gamma}\left(\frac{\omega_1^2(\vec{r})}{\omega_1^2(\vec{r})+2\delta^2}\right)^3(\alpha\cdot v)\alpha, \quad (24)$$

where $\alpha = \nabla\omega_1(\vec{r})/\omega_1(\vec{r})$.

For very cold atoms and small Doppler shift $kv \ll \Gamma$, J. Dalibard derived an expression for the dipole force in a quasi-classical approximation. According to his results at positive laser frequency detuning $\delta > 0$ the gas of atoms cools down while the dipole force pushes it out of a high field region, where the scattering force is smaller than the dipole one. Negative frequency detuning $\delta\nu > 0$ leads to heating of atoms, the atoms are accelerated and drawn to the high field region.

3.5. Subdoppler cooling

In 1989 theorists have proposed some models to explain the observed experimental results on subdoppler laser cooling. It turned out that the Doppler limit can be overcomed. To achieve the temperature much lower than the Doppler limit is possible when the nonadiabatic effects are large for the atom moving in a standing wave.

It means that the internal state of the atom changes significantly during its motion in a standing wave. If the radiative lifetime of the excited state $\tau_R = 1/\gamma$ and the optical pumping time $\tau_p = 1/\gamma\prime$, where $\gamma\prime$ is the width of the ground state, then $\tau_p \gg \tau_R$ and $\gamma \gg \gamma\prime$. Also at small intensity Rabi frequency $\Omega \ll \gamma$. Therefore the nonadiabatic effects can appear at $kv \sim \gamma\prime$ that is much smaller than the velocity capture range of Doppler cooling $kv \sim \gamma$.

Consider two counterpropagating waves which form a standing wave. The amplitudes of the waves are equal, their polarizations $\vec{\epsilon}_x$ and $\vec{\epsilon}_y$ a linear and mutually orthogonal. The total field of the standing wave is the vector sum o $\vec{\mathcal{E}} = \vec{\mathcal{E}}_1 + \vec{\mathcal{E}}_2$, where

$$\vec{\mathcal{E}}_1 = \mathcal{E}_0\vec{\epsilon}_x(e^{ikz-i\omega_L t} + e^{-ikz+i\omega_L t}) \quad (25)$$

is the electric field of the first wave

$$\vec{\mathcal{E}}_2 = \mathcal{E}_0\vec{\epsilon}_y(e^{-ikz-i\omega_L t} + e^{ikz+i\omega_L t}) \quad (26)$$

is the electric field of the second wave. Their sum has the following form

$$\vec{\mathcal{E}} = 2\mathcal{E}_0\cos(kz)(\vec{\epsilon}_x+\vec{\epsilon}_y)\cos(\omega_L t) + \quad (27)$$

$$+2\mathcal{E}_0\sin(kz)(\vec{\epsilon}_x-\vec{\epsilon}_y)\sin(\omega_L t)$$

One can see from (27) that the polarization $\vec{\epsilon}_1 = \vec{\epsilon}_x + \vec{\epsilon}_y$ is linear at $z = 0$, circular σ_- at $z = \lambda/8$. At $z = \lambda/4$ the polarization is again linear $\vec{\epsilon}_2 = \vec{\epsilon}_x - \vec{\epsilon}_y$, at $z = 3\lambda/8$ - circular σ_+ and so on.

In Fig.5 the energy of an atom is shown. The atom moves in a low intensity standing wave. The levels $g_{-1/2}$ and $g_{+1/2}$ are ground states with the magnetic quantum numbers $m_J = -1/2$ and $+1/2$ respectively. The energy of each level changes periodically in space due to its interaction with the laser wave (dressed states). Shift of the atom energy, which appear as a result of this interaction, is called light shift $\triangle E_0$. Various sublevels have different light shift at a given point of space, because the energy interaction between a photon and electron in a given quantum state depends on the magnetic moment of the photon (or the wave polarization).

The probability of atom transition between ground g and excited e states is proportional to the squared Clebsh-Gordan coefficient for the corresponding levels, these coefficients are shown in Fig.6 for various Zeeman sublevels.

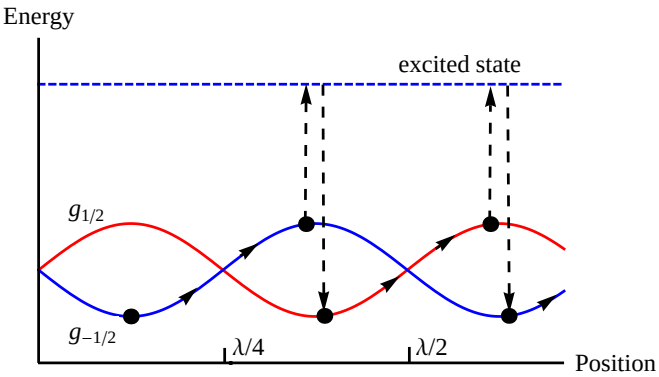

FIG. 5: Laser cooling by the method of polarization gradient. The energies of the ground states $g_{1/2}$ and $g_{-1/2}$ in the standing wave depending on the atom position, λ is the wavelength.

The atoms are translated from one ground state sublevel to one of sublevels of an excited state during the optical pumping time $\tau_{\rm opt}$. The probability of photon absorption is the largest at maximal value of energy. At properly selected time of optical pumping $\tau_{\rm opt} \sim \lambda/(4v)$ and $\tau_{\rm rad} \ll \tau_{\rm opt}$ atoms cool down in the standing wave, because the atom climbs the hills of potential energy more often than goes down losing the energy.

Obviously the minimum temperature in this method is determined by changing potential energy of an atom moving in the standing wave. The maximum change called light shift is

$$\triangle E_0 \simeq k_B T_{\rm min}. \quad (28)$$

For small recoil energy and light shift much smaller than the energy width of the excited state $\hbar\Gamma$ it is possible to get the temperatures of the micro Kelvin range

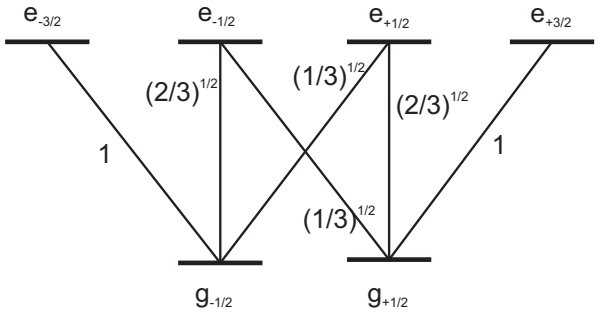

FIG. 6: Clebsh-Gordan coefficients for the transitions between various sublevels of ground g and excited states for the case when the total angular momentum of the ground level is $j_g = 1/2$ and the angular momentum of the excited level is $j_e = 3/2$.

[53, 109]. So at decreasing intensity of light wave the temperature of atoms decreases also until it reaches some limit determined by single-photon recoil energy $E_{\rm rec}$ (36)

$$T_{\rm rec} = \frac{\hbar^2 k^2}{2Mk_B}, \tag{29}$$

where M is the atom mass. The limitation arises, because the last spontaneously emitted photon has a finite momentum $\hbar k$. The subdoppler cooling works effectively due to the dipole force in a near-zero velocity range [77]. For sufficiently large velocities it becomes ineffective, and the Doppler cooling comes into play. The both methods may be used for laser cooling of antihydrogen.

To get the temperatures below the Doppler limit is possible in a standing wave, but neither with $\sigma^+ - \sigma^-$ configuration nor with classical molasses.

According to the of subdoppler cooling [77] the temperature of atoms depends on detuning in the following way

$$T = C\frac{\hbar\omega_1^2}{|\delta\nu|k_B}, \tag{30}$$

where $C = 1/8$, ω_1 is Rabi frequency, $\delta = \omega_L - \omega_0$ is frequency detuning. This theoretical behaviour agrees with the experiment [83].

It is known that from the experiments with laser waves of parallel polarizations the coefficient equals $C_\parallel = 0.45$ [83], and for perpendicular laser polarizations $C_\perp = 0.35$ [83] obtained for six laser beams. The theory of cooling predicts $C_\perp = 0.13$ for two counterpropagating waves [77]. The experiments showed that the minimum achievable temperature is also proportional to the intensity of a laser wave [83].

In a magnetic trap the rate of laser cooling depends on the magnetic field. This dependence is easily explained by Zeeman shift of atomic levels. To get effective cooling in the magnetic field the Zeeman splitting and shifts of the levels in a magnetic field should be taken into account when we choose an optimal frequency detuning [53]. Neglecting the effects of magnetic field causes to slow cooling and spurious optical pumping into untrapped states.

4. REVIEW OF EXPERIMENTS

4.1. Precision measurements. Spectroscopy.

A great work has been already done and the incredible precision was achieved in measurements of atomic hydrogen spectrum. With an improved detection method the frequency of $1S - 2S$ transition was obtained with a relative accuracy 4.5×10^{-15} and it equals to 2466061413187018(11) Hz [110]. The $1S$ ground-state Lamb shift in hydrogen atom was measured in 1992 with the relative accuracy equal to 1.3×10^5 and its value is 8172.82(11) MHz [111], the experiment was performed at room temperature by Doppler-Free Two-Photon spectroscopy. The frequency of $GS - HFS$ splitting of $1S$ level in hydrogen atom is known with 6.3×10^{-13} and equals to 1420405751.7667(9) Hz [112], $2S$ hyperfine interval has a value 177556834.3(6.7) Hz [113].

There is a hypothesis about a drift of coupling constant α in time [114] based on astronomical observations of spectral lines [115]. Annual measurements of atomic transition frequencies make possible to determine a change of the coupling constant α [116]. If this change is not zero then in accordance with the Grand Unification Theory other physical coupling constants are also changing in time. However such changes of fundamental constants are forbidden in theories with a metric including general theory of relativity, because it violates the Einstein's equivalence principle.

Previous data on the $1S - 2S$ transition frequency [117, 118] allow to set a limit on the α coupling constant drift. The drift equals to $(3.2 \pm 6.3) \times 10^{-15}$ per year, i.e. zero in the range of errors. The precision spectral measurements of hydrogen and antihydrogen are important because they could set a limit on an applicability of modern physics laws. The results were obtained by use of the optical frequency comb formed by a femtosecond laser. Optical combs lead to a revolution in a high precision measurements, for detailed study we recommend a review [119].

The one of the primary goals of $CERN$ collaborations is a high precision laser spectroscopy of antihydrogen atom. Today the accuracy of such experiments is low, experimentalists have to work with small amount of antiatoms. The problems are often associated with the arrangement of an experimental setup. For example $ALPHA$ collaboration has measured the ground-state hyperfine splitting ($GS - HFS$) of antihydrogen atom [120]. To avoid a loss of antiatoms due to annihilation the experiment was done in the magnetic trap with the depth 0.5 K. The experimental measurements were performed with the relative accuracy 3×10^{-3}. There are various uncertainty sources such as the low statistics, magnetic

field of the trap, etc.

Hyperfine splitting of energy levels is mainly a magnetic effect and occurs due to the interaction of the magnetic moments of positron and antiproton. To achieve a high precision in study of the ground-state hyperfine splitting the magnetic field should be absent. It was suggested to use a "cusp" configuration of magnetic fields for the synthesis of atomic antihydrogen and further spectroscopic measurements [121]. The scheme is described in [122, 123]. Coalescence of positrons and antiprotons occurs in-flight and the spin-polarized beam of antihydrogen atoms goes out of the cusp trap. Using this method $ASACUSA$ collaboration obtains in $5-50$ times larger antiatoms than in experiments of $ATRAP$ and $ALPHA$ during one working cycle of antiproton decelerator [121]. In the radio-frequency quadrupole decelerator ($RFQD$) antiprotons are slowed down to 115 keV before a movement to the cusp trap for the antihydrogen synthesis. To increase the production of antitoms the rf-drive is applied to antiprotons. It turns possible to get 25 antiatoms per hour with the principal quantum number $n \lesssim 29$ for number of antiprotons 5×10^7 coming from Antiproton Decelerator. ASACUSA aims to measure the $GS-HFS$ splitting of antihydrogen using a beam of antiatoms from the cusp trap [124].

Laser cooling could help to improve an accuracy of some experiments on the spectrum of hydrogen and antihydrogen. Modern Doppler-Free spectroscopy avoids errors due to the first-order Doppler broadening. But there is the second order Doppler effect, which shifts a spectral line, changes its shape and degrades an accuracy of experiments. If measurements are performed in a magnetic trap, the external magnetic field leads to the magnetic broadening of the spectral lines. The colder atoms localize in the region of the trap with the weaker field, thus the accuracy of the experiment is higher.

As a powerful source of Lyman radiation is not still created, the experiment with a beam of antimatter seems more promising, since the measurements can be performed in the absence of the magnetic field. Powerful laser radiation could also be used for collimation of an experimental beam, see Section 8.

At high temperatures the energy exchange can occur between internal and external degrees of freedom in an atom owing to collisions, which also leads to a shift of atomic energy levels. At thermal energies the level broadening $\triangle\nu \sim n\sqrt{T}$, where n is the concentration of atoms, T is the temperature. For number of antihydrogen atoms which we have in the experiment this broadening is absent.

The number of antiatoms has to be increased. Typically, the spectroscopic measurements are performed with millions of neutral atoms within fractions of a second, or about a second. If the number of antiatoms would be the same as in experiments with usual atoms, then the spectra have been able to measure during the dispersion with a high precision. We do not have so many antiatoms. However, scientists have learned to keep antiahydrogen in the magnetic trap of superconducting type ~ 1000 s at the number of antiatoms of a few hundred. It would be desirable to increase by two orders of magnitude either the retention time or the number of antiatoms. $ELENA$ experimental facility would lead to an increase of antihydrogen yield.

4.2. Experimental check of Einstein's equivalence principle

Another research area in antihydrogen physics is the check of Einstein Equivalence Principle, the basis of theory of general relativity. The observed acceleration of Universe expansion causes many fundamental questions as our understansing of the gravitation is incomplete.

There are many compelling arguments which confirm the equality of gravitational and inertial mass of matter and antimatter, but they are indirect and based on theoretical assumptions such as CPT theory and Lorentz invariance.

$ATRAP$ collaboration found the ratio of gravitational mass to inertial mass $F < 200$ at 2σ level [125], the measurements were performed in the magnetic trap. The next experiment of $ALPHA$ collaboration showed that $-65 \leq F \leq 110$ at a statistical level of significance equal to 95% [126]. It is also affirmed in this work that cooling the antiatoms to temperatures ≤ 30 mK and increasing the shut-down time of the magnetic field in the trap makes possible to measure the ratio F with ± 1 accuracy.

The frequency analysis of the non-linear antihydrogen dynamics in magnitostatic trap has been done in [127] using numerical methods. It was shown that stochasticity is insufficient and ergodicity is not satisfied for the antiatom motion in the magnetic trap because radial and axial motions of antiparticles are uncoupled. The accuracy of F determination strongly depends on the shut-down profile of the radial field component. The requirement of ergodicity is essential assumption for the gravitational experiments carried out by $ALPHA$ [126] and $ATRAP$ collaborations [125].

Collaboration $AE\bar{g}IS$ proposed to measure the gravitational acceleration of antihydrogen using the shift of interference fringes created by antiatom beam [128–130]. Atomic antihydrogen is synthesized via resonant charge-exchange collisions of Rydberg Ps^* with antiprotons at temperature 100 mK, the number of 10^5 antiatoms is needed to obtain $\bar{g}$ with 1% accuracy.

Collaboration $GBAR$ also produces antihydrogen atoms via a resonant charge-exchange collisions but their in-flight measurement of g-value demands much lower atomic velocities of the order of m/s or temperatures $\sim 20\,\mu$K. Antihydrogen ions $\bar{H}^+$ are produced through the reactions

$$\bar{p} + Ps^* \rightarrow \bar{H} + e^-, \tag{31}$$

$$\bar{H} + Ps^* \rightarrow \bar{H}^+ + e^-. \tag{32}$$

Then $\bar{H}^+$ are sympathetically cooled by beryllium ions to μK temperature range. The second positron is photodetached and the antiatoms fall down on the detecting plate, where the annihilation takes place. This production scheme is complicated so the $\bar{H}$ yield is low. Experimentalists aim to obtain antihydrogen atoms initially at temperatures $\sim \mu$K.

$GBAR$ also plans to measure the gravitational levels of antihydrogen like for the neutron [131]. The advantage is that antihydrogen atoms are detected much better than neutrons. The spectroscopy of gravitational levels could improve the accuracy of $\bar{g}$ measurement [132].

Check of electrical neutrality is very important for the proper interpretation of gravitational experiments. Surrounding electric fields prevent such experiments with charged particles. The gravitational forces exceed the electrical ones when the electrical charge of the $\bar{H}$ is less than $10^{-7}e$. Results of $ALPHA$ collaboration show that this condition is satisfied [133].

$ALPHA$ collaboration set a bound on the electrical charge of antihydrogen [133]. It equals to $Q = (-1.3 \pm 1.1 \pm 0.4) \times 10^{-8}$ with a statistical confidence level of 1σ, the first error is large and caused by small statistics, the second one is the consequence of systematic effects. Modern experiments show that ordinary matter is neutral with the accuracy equal to $(-0.2 \pm 1.1) \times 10^{-21}e$ [134] and the same has to be true for antimatter.

4.3. Bose-Einstein Condensation

It was shown in 1976 with many body calculations [135] that spin-polarized atomic hydrogen retains its gaseous properties at all temperatures. In 1980 at Amsterdam the spin-polarized H was obtained in experiment by W. Silvera and J. Warlaven [136]. Bose-Einstein condensation of spin-polarized atomic hydrogen is of great interest because the interaction between atoms is very weak, so the measurements of the BEC properties can be performed with a high precision. Using atomic hydrogen makes possible to check the theories of condensates and the theory of ultra-cold collisions, explore spin-waves, collective phenomena, correlations, quantum phase transitions, etc.

Upon reaching the temperatures of the order of microKelvin the experimentalists also have an access to quantum physics with atoms. The ground state of alkali-metal atoms is the solid. It limits the lifetime of such gases and the accuracy of experiments. Hence the use of atomic hydrogen for some experiments may be more advantageous.

The transition temperature of hydrogen to BEC phase occurs at 50 μK. Alkali-metal atoms has a lower critical temperature of condensation, for example Li condenses at 0.3 μK, Na at 2 μK. Laser cooling methods allow to precool such atomic species to mK temperature range. Laser cooling till μK temperatures can be cariied out only for alkali-metal atoms, but not for atomic hydrogen mainly due to the absence of powefull Lyman-α laser sources.

Many unsuccessful attempts have been undertaken to obtain BEC phase of hydrogen in laboratory because spin-polarized atomic hydrogen recombines into a molecular state owing to the adsorption on the walls and three-body recombination. In 1986 at MIT hydrogen gas was cooled till 30 μK and density equal to 2×10^{14} cm^{-3} due to evaporative cooling and magnetic compression in a static magnetic trap [137].

Bose-Einstein condensate of atomic H was obtained in 1998 in the magnetic trap and detected using laser spectroscopy [138–140]. The temperature 50 μK and density 1.8×10^{14} cm^{-3} were achieved due to the evaporating cooling and rf evaporation. The diameter of the condensate was equal to 15 μm and its length was 5 mm. The peak condensate density was 4.8×10^{15} cm^{-3}, which correspons to 10^9 atoms.

Magnetic trap played a key role in these experiments [141]. Hydrogen atom has a non-zero magnetic moment and may exist in various spin states. Atoms in the "low-field seeking" state move to a spatial region with the smallest field value, i.e. to the center of the trap. Hydrogen is thus isolated from the chamber walls.

BEC phase of antimatter is also extremely interesting for researches. At temperatures close to zero spin-polarized antihydrogen would present an ideal system for check of quantum mechanics laws. The interatomic interactions can be calculated to a high precision. Unfortunately such low temperatures are far beyond the technical capabilities. The antimatter samples cannot be made sufficiently dense at current experimental facilities to apply evaporative cooling. The number of antihydrogen atoms obtained in a laboratory amounts to hundreds today. Therefore obtaining of $\bar{H}$ Bose-Einstein condensate is impossible without laser cooling. Indeed, unlike conventional hydrogen the antihydrogen atoms cannot be precooled by collisions with walls of a vacuum chamber, because it would lead to annihilation.

Also worth noting that the atoms in this phase are easy to control, since the scattering length depends on the external magnetic field.

4.4. Experiments on cooling of hydrogen

The first and the only experiment on optical cooling of atomic hydrogen was carried out in 1993 [144]. Hydrogen atoms were precooled by cryogenic technology to the temperatures ~ 80 mK and loaded into the magnetic trap with the well depth ~ 0.82 K. The radius and the length of the trap were 6 mm and 12 cm correspondingly.

Density of spin-polarized atomic hydrogen at the center of the trap was relatively high $n \gtrsim 10^{11}$ cm^{-3}. The magnetic field configuration in the trap was described in [144, 164–166] and its absolute value was determined by $|B(\vec{r})| = (B_\perp^2 + B_z^2)^{1/2}$, where $B_\perp \approx \alpha\rho$ is the component of the magnetic field perpendicular to the trap axis, r is

the distance from the symmetry axis, $B_z = B_0 + \beta z^2$ is the field component along the axis of the trap, z is the coordinate along this axis, $\alpha = 2.2$ T/cm, $\beta = 0.023$ T/cm^2 and $B_0 \simeq 0.1$ T is the minimum field value in the trap.

J. Warlaven and his colleges utilized the Lyman-α transition $1S_{1/2} - 2P_{3/2}$ for laser cooling. The total power of the laser source was 160 nW. The power in a region of atoms localization was equal to 2.5 nW. Atoms were irradiated by circularly polarized light, its intensity was 100 times smaller than the saturation intensity. The source generated $2 \cdot 10^9$ photons per pulse, the duration of the pulse was 10 ns, the repetition rate was 50 Hz. The bandwidth of laser radiation did not exceed 100 MHz.

Doppler cooling makes it possible to cool atoms from 80 mK to 11(2) mK temperature during 15 minutes. Cooling proceeds slowly compared to the inter atomic collisions rate which is equal to $\tau_c^{-1} \sim 0.1 - 10$ s^{-1} but much faster than the decay rate due to spin flips in the interatomic collisions $\tau_d^{-1} \sim 10^{-5} - 10^{-3}$ s^{-1}. During cooling the density of atoms increased 16 times, however 99.9994 % of particles leave the trap due to the spin flips. Thereafter the Doppler cooling was performed again at lower density. The minimum temperature was equal to 8 mK, that is slightly above the Doppler limit for the hydrogen atom. Subsequent evaporative cooling makes it possible to get even lower temperatures $T = 3(1)$ mK [137, 144].

Let's estimate the time of laser cooling in this experiment from common principles of Doppler cooling theory. The magnetic field in the trap is not uniform, so the density of atoms distributes according to the Boltzmann law and its potential energy is the function of temperature and an atom position in the magnetic trap is

$$n(\vec{r}) = n_0 \exp[-\frac{\mu_B(B(\vec{r}) - B_0)}{k_B T}], \qquad (33)$$

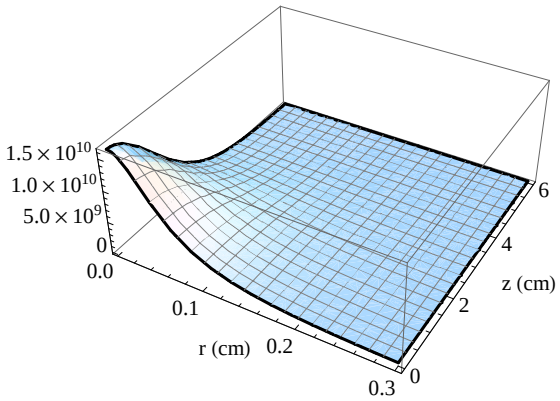

FIG. 7: Density distribution of hydrogen atoms in the magnetic trap at $T = 80$ mK, density at the trap center equal to 10^{11} cm^{-3}, r is the radial distance from the trap axis, z is the coordinate along the trap axis.

where n_0 is the density of atoms at the magnetic trap center, μ_B is the Bohr magneton, $B(\vec{r})$ is the magnetic field in the point (z,ρ). In Figure 7 we show the density distribution of hydrogen atoms at temperature $T = 80$ mK in the magnetic trap. The total number of particles amounts to $\sim 3 \times 10^9$ in the trap.

For the most efficient laser cooling the detuning δ has to be equal $-(\gamma_{sp} + \gamma_{las})/2 \approx -6.27 \times 10^8$ Hz, where $\gamma_{sp} = 6.26 \times 10^8$ Hz is the spontaneous decay rate of the $2P$ state, $\gamma_{sp} = 2\pi \times 10^8$ Hz is the laser linewidth.

Using the Doppler force acting on hydrogen atom roughly evaluate the cooling time 80 mK till 11 mK. Energy of the atom change with the rate

$$\frac{dU}{dt} = \frac{t_p}{t_R}\frac{I}{I_0}\frac{\hbar k^2/M_H}{1 + (2\delta/\gamma)^2}\left(\frac{24 k_B T \delta}{\gamma(1 + (2\delta/\gamma)^2)} + \hbar\gamma\right) \qquad (34)$$

where $k = 2\pi/\lambda$, $\lambda = 121.56 \times 10^{-9}$ m is the laser wavelength, $M_H = 1.67 \times 10^{-27}$ kg is the mass of atomic hydrogen, $k_B = 1.38 \times 10^{-23}$ J/K is the Boltzmann constant. The diameter of laser beam is equal to 2 mm. We found the cooling time equal to ≈ 10 min for the intensity in 100 times smaller than saturation intensity $I/I_0 \approx 0.01$ [144], while the experimental value amounts 15 min. The shifts of levels due to the external magnetic field have not been taken into account. The duration of the pulse $t_p = 10$ ns and its repetition rate $1/t_R = 50$ Hz. At the initial temperature 80 mK only 34.07 % of all the particles are inside the laser beam. As the temperature reduces the hydrogen atoms localise near the center of the trap and at 11 mK the laser beams covers 99.98 % of the particles remaining in the trap.

For continuous wave laser source of the power 20 nW the cooling time would be equal 110 min so the pulsed lasers are still the best choice for cooling of antihydrogen atoms. CW lasers are necessary for creation of optical molasses or beam-stopping experiments because in the pulsed irradiation with low pulse duration the atoms (antiatoms) escape simply from the volume in the time between two pulses.

5. PROBLEMS OF LASER COOLING OF (ANTI)HYDROGEN

5.1. Large Doppler limit and recoil energy

We estimate some parameters specific for the Lyman transition $1S_{1/2} - 2P_{3/2}$ in an antihydrogen atom. Using the value of the transition width, the values of Boltzmann and Plank constants we get from (13) the Doppler limit $T_{\rm dop} = 2.4$ mK for the antihydrogen atom. The average velocity of the antiatoms at this temperature $v = \sqrt{3k_B T/m_H} \approx 7.71$ m/s. In the experiment due to spatially inhomogeneous shift of Zeeman sublevels the minimal temperature is usually higher. The Zeeman shift of the energy of excited states

$$\triangle E = \pm g_J \mu_B B, \qquad (35)$$

where $m_J \neq 0$ is the magnetic quantum number, g_J is the Lande factor of the excited state, μ_B is the Bohr magneton.

For effective Doppler cooling the recoil energy $E_{\rm rec}$ should be small in comparison with the level width in energy units $\hbar\gamma$

$$E_{\rm rec} = \frac{\hbar^2 k^2}{2m_H} \ll \hbar\gamma, \tag{36}$$

where $k = 2\pi/\lambda$ is the wave vector. The inequality holds at $k\triangle v \ll \gamma$ in the semiclassical approximation implying $\triangle r \ll \lambda$ where $\triangle r$ is an atom size. Taking into account the Heisenberg ratio it's easy to verify that the expression (36) holds. We substitute the numerical values for the Lyman-α transition in (36) and find $E_{\rm rec} \approx 8.86 \cdot 10^{-27}$ J, $\hbar\gamma \approx 0.67 \cdot 10^{-25}$J, where $\hbar = 1.05 \times 10^{-34}$ J $\cdot$ s so the ratio $E_{\rm rec}/(\hbar\gamma) \sim 0.13$.

The recoil energy of antihydrogen atom for Lyman-αwavelength corresponds to the temperature $T_{\rm rec} = E_{\rm rec}/k_B \simeq 0.64$ mK, the corresponding atomic velocity is equal to 3.98 m/s. The velocity mean change after scattering of a single photon $\triangle v = 2\pi\hbar\nu/(m_H c) \approx 3.26$ m/s, where m_H is the mass of an antihydrogen atom. Large recoil energy also slows down the cooling rate and this is not good especially for antiatoms. Their confinement time is limited because of collisions between antiatoms and residual hydrogen H_2 and helium He in the magnetic trap.

All the spectrum transitions in $\bar{H}(H)$ from the ground state lie in the deep ultraviolet, and have even lower wavelengths and larger recoil energies than for the $1S - 2P$ transition. Note that for $1S \to 2S$ two photon cooling scheme the recoil temperature equals 1.2 mK [147]. Obviously the use of different spectral transitions don't help to overcome the problem. Nevertheless to cool antihydrogen atoms below the recoil energy is possible theoretically due to coherent population trapping, which has already been demonstrated for helium atoms [85, 148]. However it needs high laser power close to saturation and very narrow laser linewidth [85].

5.2. Limited optical access

In experiments atomic collisions with the walls of vacuum chamber, covered by liquid helium, assisted significantly in the achievement of low temperatures ~ 4 K. Obviously for further cooling the atomic sample should be isolated from the experimental setup. Collisions with walls of vacuum chamber promote the establishment of thermal equilibrium, but lead to recombination of atoms with the surface. So the magnetic trap is utilized to avoid a heating due to collisions with the experimental setup and losses because of recombination. It's also necessary for the obtaining of spin-polarized atoms and study of its quantum properties. But the design of the magnetic traps used for H and $\bar{H}$ permits the use of only two laser beams along one spatial axis.

Exploring antihydrogen $ALPHA$ and $ATRAP$ collaborations use superconducting octupole magnetic trap with the depth ~ 0.5 K. It isolates the antimatter from the walls of a vacuum chamber to prevent annihilation. The design of the magnetic trap for atomic antihydrogen is more complicated than for hydrogen but both belongs to the same Ioffe type. Octupole magnetic traps also assume laser cooling of (anti)atoms along the one spatial direction.

From Section 3 3.2 it follows that cooling in the longitudinal direction leads to a heating in the perpendicular ones, because atoms absorb laser photons along the beam axis, while the spontaneous emissions occur in random directions. This presents a problem in the case of low density of (anti)atoms in the trap, because its rare collisions do not provide the necessary energy exchange between various spatial degrees of freedom.

Density of antihydrogen atoms obtained at $CERN$ is very small. There is no simple mechanism which can help in achievement of thermal equilibrium because antiatoms should be isolated from the trap walls. The possible solution of this problem was proposed in [167]. It was suggested to use nonharmonic magnetic fields to improve a connection between various degrees of freedom. The use of a pulsed source of Lyman-α irradiation with the power of 0.1 mJ, pulse duration 10 ns, repetition rate 10 Hz and diameter 10 mm could give the lowest temperature ~ 20 mK.

5.3. Absence of powefull Lyman source

The lifetime of antihydrogen in a magnetic trap is not long enough because the vacuum in the magnetic trap is not ideal. So antihydrogen annihilates with the background gases which are present at the experimental setup. At high density $\sim 10^{13} - 10^{14}$ cm^{-3} the processes of spin flips or Maorana transitions come into play because of the mutual interatomic collisions [145, 146] which are relevant only for hydrogen experiment for now.

Spin flips also occurs owing to light scattering by atom and photoionization processes. Such events are undesirable and lead to a loss of (anti)particles from the magnetic trap. Because the lifetime of antihydrogen is limited to several hundreds of seconds the powefull laser sources are necessary for the rapid cooling of antiatoms.

The Lyman-α transition $1S_{1/2} - 2P_{3/2}$ in the antihydrogen atom is the best suited for the laser cooling, because $2P$ state has a shot lifetime equal to $\tau \approx 1.6$ ns. The photoionization probability of excited state $2P_{3/2}$ is small. At saturation regime the cycle absorption-emission is about 5 ns due to a very small lifetime of $2P_{3/2}$ state. Spin flips or Maorana transitions due to the light scattering also occur less frequently on this transition.

However laser sources at the wavelength $\lambda = 121.6$ nm do not have enough power for fast and efficient cooling

of (anti)hydrogen. The production of continuous irradiation is very complex and accessible power of such laser sources is very small today [142, 143]. The pulsed sources of Lyman-α irradiation has a slightly higher power than continuous one.

Let's estimate saturation intensity for $1S_{1/2} - 2P_{3/2}$ transition in antihydrogen atom

$$I_0 = \frac{4\pi^3\hbar c\gamma}{3\lambda^3}. \quad (37)$$

Its wavelength $\lambda = 121.6\,\text{nm}$, the laser frequency $\nu = c/\lambda = 2.47 \cdot 10^{15}\,\text{Hz}$ (c is the speed of light), the bandwidth of laser irradiation is equal to 100 MHz, the natural linewidth $\gamma_{sp} = 2\pi \times 10^8$ Hz. We do not consider detuning of laser wave from the $1S_{1/2} - 2P_{3/2}$ transition. For these parameters from (37) we get the value of saturation intensity $I_0 \approx 45.6\,\text{W/cm}^2$. At present time laser sources of continuous Lyman-α irradiation can reach the maximal power of $P = 200\,\text{nW}$ [143]. For the beam with the cross-sectional area $S \simeq 1.76 \cdot 10^{-2}\,\text{cm}^2$ the intensity value is

$$I = P/S = 0.6 \cdot 10^{-3}\,\text{W/cm}^2, \quad (38)$$

so the ratio $I/I_0 = 1.3 \cdot 10^{-5}$, which is not large enough for the fast laser cooling.

5.4. Generation of continuous Lyman-α irradiation

Production of the coherent Lyman-α irradiation with $\lambda = 121.56$ nm is very difficult because the non-linear crystals or tunable lasers are absent at this wavelength. The well known BBO crystal (barium borate) is the nearest to this optical region, however even BBO crystal is transparent for the wavelengths > 190 nm. In 1977 the four-wave resonant mixing in a gas was proposed for the Lyman-α irradiation. The first Lyman-α sources were pulsed and employed the Krypton gas [149–155].

Usual Lyman sources have a very small power because the generation of such irradiation by four-wave mixing is technologically difficult process. The maximum reflectivity of mirrors is equal to 85 %, the transmission coefficient of lenses is ~ 50 %. So the arrangements producing this light should contain the minimal numbers of lenses and optical elements. Laser light should spread in vacuum or He to minimize the intensity loss.

In 1999 K.S. Eikema proposed two schemes using the spectral transitions in mercury vapour for obtaining the cw Lyman-α emission [156].

The first scheme is shown in Figure 8 and based on resonant transitions between several atomic levels 6^1S, 7^1S and 12^1P. They achieved the maximum power 3 nW of Lyman-α emission at 121.9 nm using three fundamental beams.

In the second scheme 6^1D and 6^3D levels were used instead of 7^1S level. It turns out that the efficiency of the second method was twice lower than of the first one. Later the power of this Lyman-α source was improved till 20 nW and spectroscopy measurements were performed on $1S - 2P$ transition in hydrogen [157].

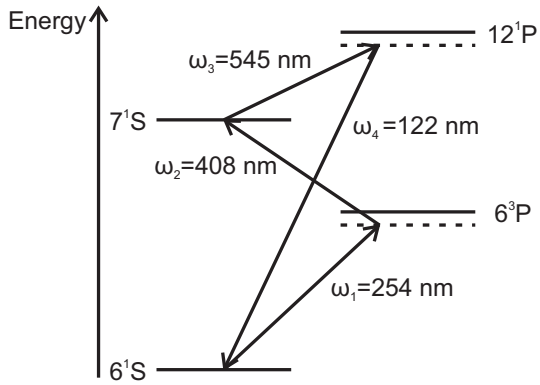

FIG. 8: Energy-level diagram of mercury levels used for generation of Lyman-α irradiation by sum-frequency four-wave mixing. Three fundamental beams at 254 nm, 408 nm and 545 nm excite the atoms from 6^1S state to 12^1P followed by the spontaneous emission of Lyman-α irradiation.

The power of Lyman-α irradiation is defined by the following equation

$$P_4 = \frac{9}{4}\frac{\omega_1\omega_2\omega_3\omega_4}{\pi^2\epsilon_0^2c^6}\frac{1}{b^2}\frac{|\chi^{(3)}|^2}{\triangle k^2}P_1P_2P_3|G(b\triangle k)|^2, \quad (39)$$

where ω_1, ω_2, ω_3 and ω_3 are the frequencies of the fundamental and generated beams correspondingly. b is the confocal parameter, $\triangle k = k_4 - k_1 - k_2 - k_3$ is the phase mismatch, N is the density of the gas, $|\chi^{(3)}|$ is the third-order non-linear susceptibility. P_1, P_2, P_3 are the powers of the fundamental beams, P_4 is the power of Lyman beam, $|G(b\triangle k)|^2$ is the phase-matching integral, ϵ_0 and c are the fundamental physical constants.

The third-order non-linear susceptibility of mercury factorizes [158]

$$\chi^{(3)} = \frac{N}{6\epsilon_0\hbar^3}\frac{\chi_{12}\chi_{34}}{\omega_{ng} - (\omega_1 + \omega_2)}, \quad (40)$$

where the partial susceptibilities are defined by the following way

$$\chi_{12} = \sum_m \left(\frac{p_{nm}p_{mg}}{\omega_{gm} - \omega_1} + \frac{p_{nm}p_{mg}}{\omega_{gm} - \omega_2}\right) \quad (41)$$

$$\chi_{34} = \sum_\nu \left(\frac{p_{n\nu}p_{\nu g}}{\omega_{g\nu} - \omega_4} + \frac{p_{n\nu}p_{\nu g}}{\omega_{g\nu} + \omega_3}\right) \quad (42)$$

The susceptibility shows the enhancement at the small value of detuning $\delta = \omega_{gm} - \omega_2$. The phase-matching integral $|G(b\triangle k)|^2$ takes its maximum value 46.3 at $b\triangle k = -4$ [159].

For the Lyman-α irradiation phase-matching can be done by changing the temperature of mercury vapour or by adding another gas, for example Kr. Usually the first way is chosen because the second one leads to the broadening of the mercury resonances and decrease of the Lyman-α yield. From 40 it follows that P_4 reaches its maximum value for $\triangle k = 0$. So one have to choose the optimum value of $\triangle k$, which depends on the experimental conditions.

The continuous irradiation is more preferable for laser cooling than pulsed one. If the laser pulse duration is t_p, the pulse repetition rate is $1/t_R$ and $t_p \ll \tau \ll t_R$ then cooling efficiency will be in t_p/t_R times lower than for the case of continuous laser radiation [109]. The cw laser irradiation has a smaller linewidth than the pulsed irradiation, this reduces the spurious optical pumping to the untrapped states during cooling process causing the loss of particles from the magnetic trap. The possible solutions of the problem of optical pumping in antihydrogen atoms were mentioned in [160]. It consists in use of circularly polarized light, a longitudinal magnetic field and a second laser with another frequency to repump the atoms via the transitions $1S_{1/2}(m_F = -1/2) \to P_{3/2} \to 1S_{1/2}(m_F = -1/2)$, where m_F is the projection of electron spin on the direction of the magnetic field [160].

In the following ten years the development of the Lyman sources has been in progress [142, 143, 161, 162]. The experimental setup from [163] is presented in Figure 9. It has several advantages in comparison with the previous arrangements for the generation of Lyman-α emission [156, 157, 161]. One of the advantages is a more powerful source of 1091 nm. The resultant emission power could be increased due to the increasing of the power of each wave in the scheme.

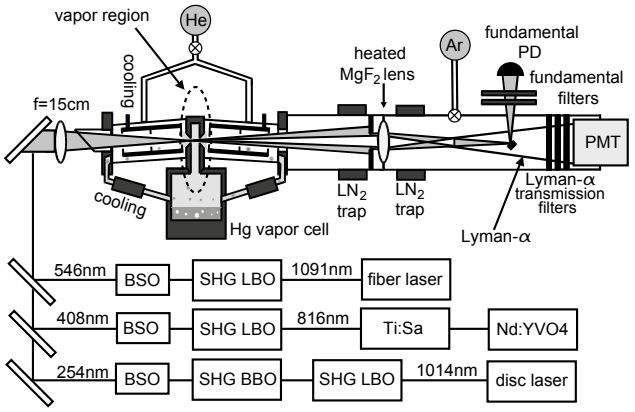

FIG. 9: The experimental setup used for the production Lyman-α emission [143]. Three fundamental beams from fiber laser, $Ti : Sa$ and disc lasers are frequency doubled in non-linear crystals (LBO and BBO) shaped by special optics (BSO) and focused in the mercury vapour cell, where the production of Lyman-α irradiation takes place. The separation of 121.56 nm light occurs due to the MgF_2 lenses and 122 nm filters. The Picture was taken from [163].

The $Yb : YAG$ disc laser generates emission at 1014 nm. Then the beam passes through a lithium triborate crystal (LBO) producing 507 nm emission and after that through β-barium borate crystal (BBO) to obtain the UV light at 254 nm. The power of the UV light may reach 750 mW if the disc laser has its maximum power 4.9 W. At such high power BBO crystal is subjected to degradation so the work power is limited to 2 W.

The second beam at 408 nm is produced by the following way. $Ti : Sa$ laser pumped by $Nd : YVO_4$ laser gives the 816 nm irradiation with the power 1.6 W. From near-infrared irradiation at 816 after passing the LBO crystal we get 500 mW of blue light at 408 nm . The work output power equals 300 mW.

The third beam at 546 nm is obtained with a fiber laser system with 10 W at 1091 nm and LBO crystal. The maximum power of the third beam can reach 4 W, however to forbid the spontaneous damage of the LBO crystal the fiber laser works at 740 mW, producing the 280 mW of green light.

The beams are shaped by pairs of spherical and cylindrical lenses, overlapped with dichroic mirrors and focused by fused silica lens with focal length of 15 cm into the mercury cell, where the four-wave frequency mixing takes place. The pressure in the mercury cell is supported at 10^{-7} mbar to prevent the absorption of UV light. The mercury cell can be heated till 240 ^{o}C and the density of atoms is 1.1×10^{24} m^{-3}. The Lyman-α yield as a function of mercury temperature is shown in Figure 10, the phase-matching temperature as a function of $6^1S - 6^3P$ detuning is also depicted for maximum Lyman-α yield [163].

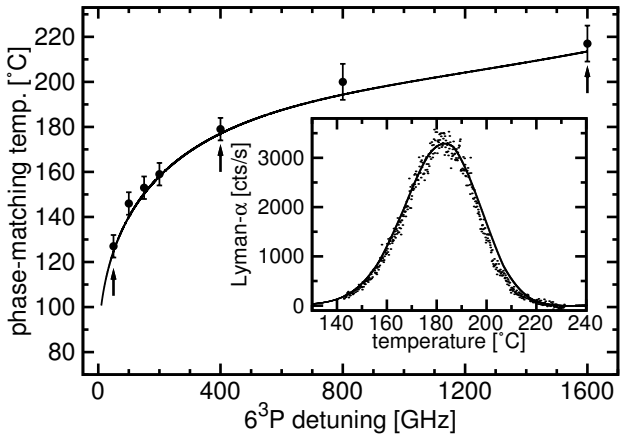

FIG. 10: The phase-matching temperature versus the $6^1S - 6^3P$ detuning. The points correspond to the maximal Lyman-αyield for various values of the detuning. Inset: the Lyman-α yield as a function of cell temperature at the detuning 400 Gz. Points denote experimental line, solid line is the fit [163].

The cooling outside the focus region is necessary to avoid the condensation of the mercury on the optics. Separating the Lyman-α emission from the fundamen-

tal beams is realized due to the MgF_2 lens. The focal lengths differ for various wavelengths. The tiny mirror behind the cell reflects the fundamental beams to the side, however it cast a shadow to the Lyman beam and produce 30% of the losses. Then the light passes through 121.56 nm filters. There is a photomultiplier tube (PMT) used for the detection of Lyman photons behind the filters. The beam of 254 nm wavelength is tuned close to 6^1S - 6^3P resonance, the blue laser (408 nm) establishes a two photon resonance between 6^1P and 7^1S state. The third beam (545 nm) is in resonance with the transition 7^1S - 12^1P. The sum-frequency gives Lyman-α wavelength at the transition 12^1P - 6^1S.

At the maximal power of the fundamental beams 750 mW, 500 mW and 4 W described system can produce Lyman-α irradiation with the total power equal to 140 nW. The increase of the yield of Lyman emission seems feasible due to increase of the transmission of the lenses and the power of the fundamental beams.

Nevertheless the generation of emission of Lyman-α wavelength is technologically complicated and the development of such lasers is a difficult task. An alternative way can consist of the use of other spectral transitions in (anti)hydrogen or other cooling methods.

6. OTHER COOLING SCHEMES FOR $\bar{H}$

6.1. Two-photon pulsed laser cooling

Theoretically it is possible to utilize other spectral transitions for laser cooling of antihydrogen atoms. However experimental attempts to do this were not undertaken. In [147] the authors discuss cw Doppler cooling of hydrogen atoms at two photon $1S-2S$ transition. The state $2S$ itself is not useful for laser cooling, because its lifetime is large 1/8 s enough, but the idea was to couple the $2S$ to the $2P$ state by a microwave radiation and the resulting state would have a much shorter lifetime. The numerical simulations show that this method allows to get the temperatures, which correspond to the recoil energy of antihydrogen for the $1S \to 2S$ transition, the Lamb shift between $2S$ and $2P$ is small and has not been taken into acoount. For the intensity $I \sim 10^3$ W/cm^2 the scheme leads to 18% ionization losses per fluorescence cycle.

It was proposed to use the ultrafast pulsed radiation [168] instead of the continuous one at 243 nm. The ultrafast pulsed radiation from the mode-locked laser has several advantages. It is a high spectral resolution and scaterring rate larger by a factor of $\sim 10^4$ than its value for the cw case. The peak power of such lasers are also higher than the power of continuous wave lasers, for example pulsed $Ti:Sa$ laser has a power up to 1 W. The restriction for the maximum used power is defined by one-photon ionization from excited state leading to losses of (anti)atoms from the magnetic trap. The scaterring rate defines the efficiency of laser cooling, its high value gives a much faster cooling.

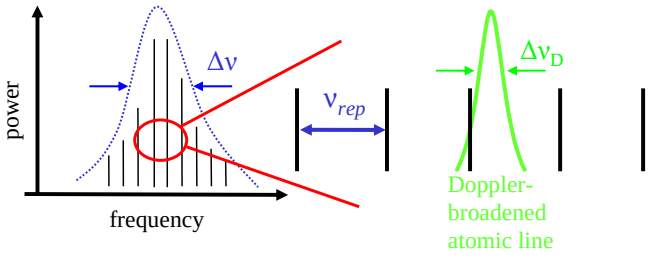

FIG. 11: Left: Power of the spectrum lines of the ultrafast pulse versus the frequency of the line. Right: Several lines of the pulse spectrum and the Doppler-broadening atomic transition of width $\triangle\nu_D$ [168].

The pulse of the ultrafast laser is a comb of sharp lines, the frequency of the line is $\nu_k = \nu_0 + k\nu_{rep}$, where k is the integer number, k_0 is the optical carrier frequency, ν_{rep} is the repetition rate. The velocity-selective scaterring takes place if one of the comb lines is resonant with the atomic transition as it is shown in Figure 11 [168]. If the Doppler width of the line is Γ_D and $\nu_{rep} \gg \Gamma_D$ then scattering rates on the other spectrum lines are reduced in $(\Gamma/\nu_{rep})^2$ times and the near-resonant line of the comb gives the dominant contribution. As a result the continuous wave laser cooling is less effective than two-photon cooling, because only one line of the comb in resonance with the atomic transition. During the two-photon process all the comb lines give significant contribution to the scattering because the transition pathways of the photons add coherently.

The possible excitation scheme for the laser cooling of (anti)hydrogen in the magnetic trap is depicted in Figure 12 [168]. The light from the pulsed laser source is tuned to the $1S-2S$ spectral transition for antihydrogen atom. The meastable $2S_{1/2}$ with $m_F = 1/2$ state quenches to the $2P_{3/2}$ state with $m_F = 3/2$ by microwave irradiation with frequency $f_{\rm micr}$ and circular polarization σ^+. The splitting of the (anti)hydrogen sublevels are very sensitive to the value of the trap magnetic field, so the frequency of the microwave irradiation have to be chosen appropriately. For zero magnetic field it would be equal to 10 GHz, at 1 T the frequency $\sim$ 20 GHz. So the light excites the atoms from the ground state $1S_{1/2}$ with $m_F = 1/2$ to some stretched state which is a superposition of $2S_{1/2}$ and $2P_{3/2}$ states and can survive in the magnetic trap. Then atoms irradiate Lyman-α photon and come back to the ground state.

For efficient two-photon process on $1S-2S$ transition we need powerful laser source, the upper limit for the intensity of the pulsed laser source comes from the one-photon ionization rate from the excited state by 243 nm irradiation. Nevertheless we think that this scheme may be a good alternative to Lyman-αlaser cooling of antihydrogen to milliKelvin temperature range. Numerical simulations showed that for the power 1.6 W of the

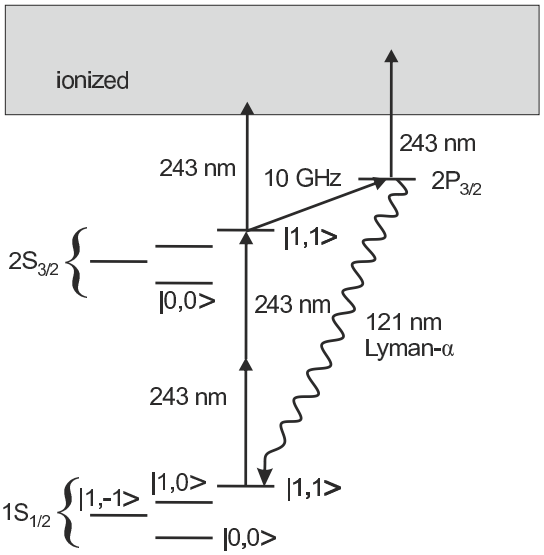

FIG. 12: Excitation scheme for laser cooling of magnetically trapped (anti)hydrogen. The two-photon pulsed laser irradiation at 243 nm excites the atoms from the ground $1S_{1/2}|1,1\rangle$ state to the $2S_{1/2}|1,1\rangle$ state. Microwave irradiation at 10 GHz quenches $2S_{1/2}|1,1\rangle$ state to the $2P_{3/2}|2,2\rangle$ state. Atoms irradiate spontaneously Lyman-αlight and come back to the ground state $1S_{1/2}$, F is the magnetic quantum number, m_F is its projection [168].

quenching irradiation and 60 kW/cm^{-2} the ionization losses consist 5%, i.e. they are less than for cw case.

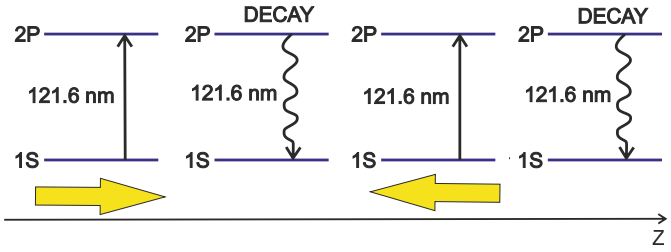

FIG. 13: One cooling cycle, consisting of a $1S-2P$ transition due to an application of the π pulse with negative frequency detuning δ in the positive direction and a spontaneous emission $2P-1S$, the use of the π pulse in the negative direction and the same transitions.

6.2. Laser cooling by π pulses

Radiation cooling by π pulses was suggested on the hydrogen Lyman-α transition in [169]. The train of coherent pulses in the opposite directions irradiate the cooling volume. The pulse train is short in comparison with the radiative lifetime of the transition. The photon from the wave moving from the left is absorbed, exciting the atom to the upper $2P$ level, followed by the spontaneous emission to the ground state $1S$, see Figure 13. To retard the motion this pulse should be detuned above the resonance. Then the pulse from the wave moving from the right is absorbed, the wave frequency is shifted below the $1S-2P$ transition. During the cooling a spontaneous emission does not occur. To escape the phase disparity the specific zero-field period is necessary between π pulses. The numerical analysis of rate equations showed that the rate of this cooling method is larger than for Doppler cooling, but it can be reached at the expense of considerably higher average power density.

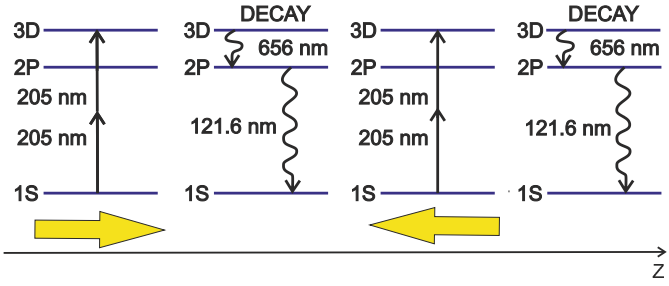

FIG. 14: One cooling cycle consisting of a $1S-3D$ transition due to the application of the π pulse with negative frequency detuning δ in the positive direction and spontaneous $3D-2P$ and $2P-1S$ emissions, the use of the π pulse in the negative direction and the same transitions.

Another scheme for laser cooling of H with π pulses was suggested in [170]. The scheme utilizes the pulsed radiation at a wavelength longer than the Lyman-α radiation. Powerful laser generates π pulses at the wavelength 205 nm and establishes the two-photon resonance with the transition $1S-3D$. Then the excited atom come back to the ground state emitting the photons at 656 nm and 121.56 nm wavelengths. Simulations showed that the final temperature achieved with a monochromatic light consisting of pulses with the duration 10 ns and the power 100 kW is close to the recoil temperature for Lyman-α transition of hydrogen ~ 0.55 mK. The limiting factors in this scheme are the very low diffusion coefficient on the $3D-2P$ transition and the recoil limit on the $2P-1S$ transition. Because of the spurious ringing effects this method might be applied only as a final step to H atoms precooled via another method.

However all these methods suffer from ionization losses which should be mitigated when we deal with small amounts of antiatoms in a magnetic trap. The first attempt to do this has been made in [171]. The scheme supposes the use of nanosecond-pulsed laser at 243 nm for $1S-2S$ two photon transition and continuous wave laser at 656 nm for $2S-3P$ transition in antihydrogen. The atoms are excited selectively depending on their velocity, which is defined by spatial atom position in an optical lattice created by cw laser waves. The scheme presents a combination of pulsed Doppler and Sisyphus cooling schemes. The minimal temperature is 1.8 mK.

Spin-flip transitions from the $3P$ excited state are suppressed in a high magnetic field.

6.3. Boofer cooling of (anti)hydrogen

The large recoil energy of the (anti)hydrogen impedes reaching temperatures below mK in laser cooling. Evaporative cooling leads to the loss of particles and progresses slowly, because the cross section of elastic scattering between hydrogen atoms has a small value.

Adding impurity atoms with a large cross section in a cooled gas can lead to a more rapid energy exchange between hot and cold atoms and serve as a source of thermalization. Laser is used for cooling of the impurity atoms which collide with the main gas and take away their energy access due to these collisions.

Thermalization rate depends on the cross section of the colliding atoms, their masses and densities. The energy exchange goes faster for the lighter atoms of the buffer gas. Boofer cooling is not dependent on internal states of the atoms. It works for the all kinds of paramagnetic species including molecules. The boofer and cooled gases has to be trapped to isolate the system from the walls of a vacuum chamber. At first the technics of boofer cooling for neutral atoms was described in 1995 [172] and performed in 1999 [173].

The boofer cooling of hydrogen was proposed in [174, 175]. This idea belongs to Professor D. Kleppner and Professor J.M. Doyle. To prevent the coalescence of different atoms and their loss from the trap the scaterring length has to be positive value. It is satisfied if the collisions occur mainly in the triplet channel ie for spin-polarized atoms [175]. The atomic cloud with a given polarization can be created in a magnetic trap with a fairly smooth magnetic field. The shape of the singlet and triplet potentials are discussed in [175]. Singlet potential has a deep minimum and triplet potential may have not such clear minimum.

Therefore the interaction can occur both in the singlet and triplet channels. When the spins of colliding atoms are parallel the atoms interact in the triplet channel, antiparallel - in the singlet one. Generally for not polarized spins the collisions occur in the singlet state. It can result to the coalesence of atoms, formation of bound states, spin flips, which in turn leads to a loss of atoms from the magnetic trap.

The method of buffer cooling suggested in [174, 175] is as follows. A small amount of cold alkali-metal atoms is mixed with hydrogen atoms in a magnetic trap. The boofer gas can be presented ^{23}Na, ^{39}K, ^{87}Rb, ^{133}Cs atoms or ^{7}Li isotopes. At temperatures considered the scaterring takes place in s-wave. Fermions ^{6}Li cannot be used as boofer gas for cooling because the s-wave scaterring is forbidden for them.

For energies $\lesssim 3$ mK the cross section $\sigma = 8\pi a_{H-H}^2$ for hydrogen-hydrogen and $\sigma = 4\pi a_{A-H}^2$ for alkali-atom-hydrogen collisions, where a_{H-H} and a_{A-H} are the corresponding scaterring lengths. Triplet cross section for $^{7}Li - H$ case is approximately 1467 larger than for hydrogen atoms. The ultracold cross section for the $Rb-H$ purely spin-polarized pairs is 860 times larger than for $H - H$ interaction. The cross section between Na and H atoms is 640 times larger than for the pair of hydrogen atoms. The interaction potential and corresponding scaterring lengths in singlet and triplet channels between various atoms and hydrogen are known and were calculated in [175] by various methods.

The large cross section between alkali-metal and hydrogen atoms might lead to a more effective evaporative cooling. Evaporative cooling can be applied for obtaining of Bose-Einstein condensates. To separate hydrogen from alkali-metal atoms one can use the microwave irradiation which produces spin flips of boofer atoms.

In the limit of low temperatures the triplet scattering length for hydrogen atoms is $a(H - H) = 1.2$ bohr, for lithium and hydrogen atoms $a(^{7}Li - H) = 65$ bohr. For lithium atoms the scattering length is large and negative $a(^{7}Li - ^{7}Li) = -27.6$ bohr, thefore the lithium atoms coalesce with each other. Such behaviour presents a problem because one can not make an experiment at large lithium concentrations. The choice of the most suitable experimental parameters, at which the cooling proceeds effectively, can be very important. The numerical simulations of particles dynamics are relevant. Therefore a small admixture of lithium atoms can speed up the process of cooling hydrogen, but their high density probably leads to a loss of particles out of the trap.

It would seem the technique of buffer cooling does not work with antimatter due to annihilation. Nevertheless P.K. Sinha and A.S. Ghosh [176] explored the interaction dynamics for $\bar{H} - Li$ system at temperatures from pK to 32 K and conclude that the ^{7}Li gas can be used for boofer cooling of atomic antihydrogen also. The sign of the interaction potential between antihydrogen and lithium depends on the temperature and on the quantum number of an antihydrogen state. For the antihydrogen in the ground state the potential is repulsive but for $n > 6$ it stays attractive from 0 to 3 K [176]. Higher excited states has no qualitative effect on the behaviour of interaction potential, however lead to an increase of the cross section and shift of the potential curve to the region of higher energies. Lithium has a large dypole polarizability in comparison with antihydrogen atoms, so the van der Waals force mainly determines the low energy behaviour.

Recently scientists suggested a method to escape annihilation. $GBAR$ collaboration plans to synthesize the positively charged ions of antihydrogen, mix them with positive charged beryllium ions, cooled by laser irradiation. The Coulomb interaction will impede annihilation. It is planed to achieve the temperatures $\sim 20\ \mu$K. Unfortunately the output of antihydrogen ions is several orders less than antihydrogen atoms.

6.4. Sympathetic cooling of antihydrogen ions

GBAR collaboration at *CERN* [177, 178] suggested not to cool the antihydrogen but obtain it in a very cold state. In their scheme antihydrogen is obtained due to the photodetachment of positron from antihydrogen ion $\bar{H}^+$ by the laser irradiation at the wavelength 313 nm. Antihydrogen ions is produced through the reaction of proton with Rydberg positronium

$$\bar{p} + Ps^* \rightarrow \bar{H} + e^- \tag{43}$$

and the reaction of antihydrogen with the positronium

$$\bar{H} + Ps^* \rightarrow \bar{H}^+ + e^-. \tag{44}$$

However the yield of antihydrogen ions in the ground state is very small. It was proposed to excite the positronium to the $3D$ level in the first reaction. It leads to the increasing of $1S$ $\bar{H}$ production by a factor of 3 [179, 180] in comparison with the positronium in $2P$ state.

The antihydrogen ions will be captured and decelerated to 10 eV. Then they will be sympathetically cooled by Be^+ ions. At first berillium ions in turn will be subjected to the Doppler laser cooling. The ions of alkali-earth elements could be easily cooled to μK temperatures. Be^+ ions is the most light alkali-earth metal with Doppler limit equal to 0.5 mK. At this temperature Coulomb repulsion is strong enough in comparison with their kinetic energy and beryllium ions are organized in Wigner crystal. After that $\bar{H}^+$ ions will be transferred to the precision trap for further sympathetic cooling, where berillium ions will be cooled by Raman sideband cooling technique to the neV energy.

To know the cooling time of $\bar{H}^+$ is very important because of possible positron photodetachment by the laser light. The lifetime of $\bar{H}^+$ is less than second under conditions of the *GBAR* experiment [181]. The computer simulations [181] has shown that the efficient and fast sympathetic Doppler cooling of energetic antihydrogen ions is possible in the presence of HD^+ ions. The cooling rate depends on the mass ratio and HD^+ ions act as a conduit between beryllium and antihydrogen ions. Raman cooling is possible within the time less than one second [181].

The Figure 15 shows the electronic Be^+ levels and illustrates the idea of Raman sideband cooling. Doppler and repumping transitions are also indicated.

The idea of the Raman sideband cooling consists in a decrease of the vibrational number of the ground state atom, when it is in the potential of the magneto-optical trap [44, 182]. Cooling is possible if the laser linewidth and the recoil energy is smaller than the separation of the atomic energy levels. Counter-propagating laser π pulses induce the Raman transitions between $|F = 2, n\rangle$ and $|F = 1, n-1\rangle$ states followed by spontaneous Raman transitions from $|F = 1, n-1\rangle$ to $|F = 1, n-2\rangle$. Repeating this procedure one can prepare Be^+ ions in the fundamental state. Elastic interactions with antihydrogen ions will transfer the kinetic energy from $\bar{H}^+$ to laser cooled beryllium ions.

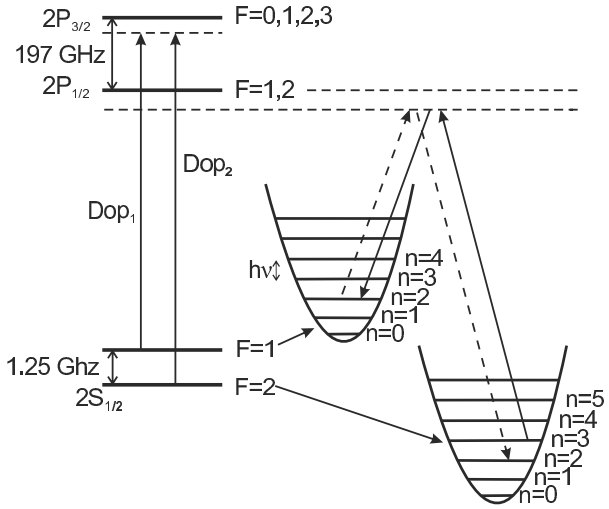

FIG. 15: Energy levels of Be^+ including the harmonic oscillator energy at the ground levels in the magnetic trap. The solid arrows indicate the stimulated Raman transition and the dashed arrows the spontaneous Raman transition. Dop_1 and Dop_2 are the Doppler cooling and repumping transitions [181].

Negative osmium ions has a bound electric-dipole transition and they can be laser cooled to the sub-mK temperature range. The sympathetic cooling of the antiprotons by osmium ions was suggested in [41]. These cold antiprotons could be used for the synthesis of cold antihydrogen by resonant charge-exchange with Rydberg positronium.

7. COLLIMATED ATOMIC BEAMS

Several experiments at *CERN* use the beam of spin-polarized antihydrogen atoms formed in the cusp trap. *FLAIR* collaboration in *GSI* will utilize such beam not only for precision spectroscopy measurements but also for experiments on study of antihydrogen collisions with other particles. In particular, a great interest presents an exploration of interaction between atomic antihydrogen and hydrogen, molecules and heavy atoms from both theoretical and practical point of view. These investigations could give signatures of annihilation between antimatter and matter in a cosmic space.

FLAIR will study the interaction potential between atomic antihydrogen and atoms and molecules, annihilation processes and formation of positronium and antiprotonic atoms, search for scattering resonances and excitation exchange between $\bar{H}^*$ and H. Interaction between excited $\bar{H}^*$ and matter has a practical importance because antihydrogen is formed in a highly excited states, it

hinders cooling and precision spectroscopy of $\bar{H}$, a study of antihydrogen dynamics in such mixtures is important.

The interaction with positronium target is of great interest because it leads to the formation of $\bar{H}^+$ and opens up the new possibilities in production of antihydrogen molecules due to associative detachment. In all these

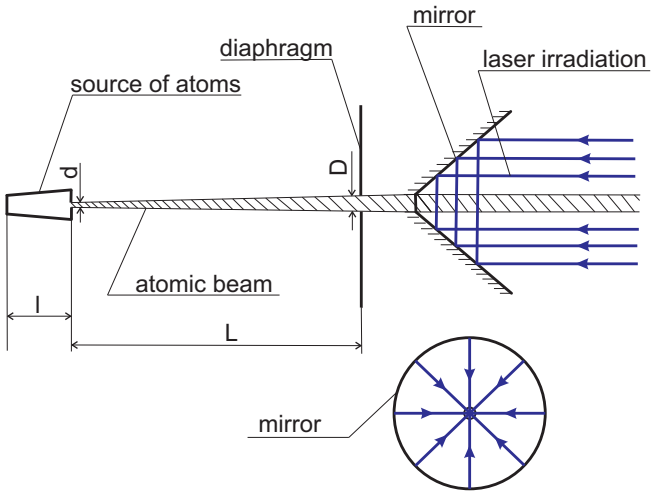

FIG. 16: The scheme of radiational collimation of an atomic beam due to the Doppler colling in the perpendicular direction to the axis of the beam.

experiments it is very important to have a collimated beam of high quality. Theoretical and experimental investigations showed that such collimation could be done by radiation pressure of light irradiation [52, 95, 183].

In Fig.16 the radiational collimation scheme of an atomic beam is shown. This scheme has been used for the experiment with sodium atoms [183]. The atomic beam from the orifice of the source pass through the diaphragm and moves to a region of space illuminated by an axially-symmetrical light field. The axially-symmetrical laser field due to mirror reflection of laser irradiation cools the atoms in the perpendicular to the beam direction. The surface of mirror is a cone with generatrix which forms angle of 45 degrees with respect to the beam axis. Therefore the maximum intensity is achieved on the axis of the atomic beam and radiation pressure force is directed to the beam axis.

Beam collimation or cooling of (anti)atoms in the transverse direction is carried out due to the Doppler cooling mechanism described in Section 3 3.2. For example in experiment with sodium atoms the temperature, corresponding to the transverse motion of atoms, decreased from 42 mK to 3.5 mK during 3×10^{-5} s when the power on the beam axis was equal to $P = 60$ mWt. The resonant transition $3S - 3P$ was used for Doppler cooling.

Usually atoms effuse from the owen at some temperature T. If the Knudsen number $K = \lambda/l \lesssim 1$, where l is the length of the atomic source, λ is the mean free path of the atom, then the distribution of atoms is Maxwellian, so atoms are moving from the source with the most propable velocity $v = \sqrt{2k_BT/m}$. For the scheme at Fig.16 the divergence angle of the beam equals to $\alpha = (D - d)/(2L)$, where d is the diameter of the orifice, D is the size of the orifice in the diaphragm, L is the distance between diaphragm and the orifice of the atomic source. The angle α is small for $d, D \ll L,\ D \ll L$. Further collimation of the atomic beam by laser irradiation has to diminish the divergence of the beam.

The minimal temperature corresponding to a stationary distribution of transverse velocities in the region of collimation

$$T = \frac{\hbar\gamma}{2k_B}\left(\frac{\gamma}{|\delta\omega|} + \frac{|\delta\omega|}{\gamma}\right) \tag{45}$$

and the corresponding angle of the beam collimation

$$\theta = \frac{\sqrt{2k_BT/m}}{\bar{v}_z} \tag{46}$$

where $\bar{v}_z$ is the average velocity of atoms along the axis of the atomic beam, m is the atomic mass, $\delta\omega = \omega_l - \omega_0$ is the laser frequency detuning from the resonance atomic frequency ω_0 [52].

The laser collimation of atomic beam is usefull for spectroscopy because it can reduce the first-order and second-order Doppler shifts on the orders of magnitude. Laser light can also be used for the spatial separation of the atoms in various internal states.

8. CONCLUSIONS

Laser cooling is of great importance for antihydrogen research. A large number of experiments devoted to study of antihydrogen and antimatter are already underway in $CERN$ and planned in GSI research facility. Among their goals are verification of basic laws of nature, such as CPT symmetry, equivalence principle, study of new aspects of nuclear physics etc. Without a laser cooling of $\bar{H}$ it is impossible to achieve a high accuracy in these experiments. Today the relative accuracy of $GS - HFS$ splitting of H ground state in 10^{10} times higher than for antihydrogen, the electrical neutrality of atomic hydrogen is confirmed with 10^{-21} precision, by 10^{13} orders of magnitude better than for antihydrogen. The measurement of $1S-2S$ transition in $\bar{H}$ hasn't been made at all.

In magnetic trap used at $CERN$ the temperature of atomic $\bar{H}$ is approximately equal to 50 mK. To improve the accuracy of the mentioned spectroscopic measurements this temperature should be in 10 times lower. The gravitational experiments need temperatures of μK range. In the magnetic trap the lowest hydrogen temperatures $\sim 3 - 11$ mK were achieved only by means of laser cooling. Laser can be used for the collimation of the antiatomic beam. The Bose-Einstein condensates cannot be obtained without laser cooling technics. The study of

quantum properties both for hydrogen and antihydrogen is not possible without laser cooling.

The $1S_{1/2}-2P_{3/2}$ spectral transition in (anti)hydrogen atom is the most suitable for the laser cooling. The corresponding laser sources of the wavelength $\lambda = 121.6$ nm already exist, but their power is not sufficient for the fast and efficient cooling. The maximal power of continuous Lyman-α sources is 200 nW, the power of pulser sources 1 mW. The creation of powerfull Lyman-α sources is very important complicated technical task. The continuous sources at this wavelength could be used for experiments with magneto-optical trap.

Laser cooling has several advantages over other methods such as evaporative cooling, sympathetic cooling and cooling due to a contact with cold walls of experimental setup. Evaporative cooling leads to a loss of atoms from the trap. Sympathetic cooling of hydrogen is difficult to implement in practice, however it seems promising and possibly can be applied for antihydrogen. The cooling owing to a contact with the cold walls of vacuum chamber also leads to the undesired recombination with the surfuce and loss of atoms. The alternative way can be a use of other transitions in the antihydrogen atom or new laser cooling schemes. Several attempts in this direction have been made already.

The great experience of cooling of the neutral atoms exists, the physical mechanisms of laser cooling have been studied. The experimental results are in agreement with the known theoretical models. Many atom's species have been laser cooled, the production of (anti)hydrogen at $\sim$ mK temperature has to be the next step. Cold antihydrogen has a great importance for fundamental science. The hydrogen $1S-2S$ transition is a promising candidate for an optical clock. The search of other possible applications of (anti)hydrogen is also significant important.

9. ACKNOWLEDGMENTS

The work was carried out with the financial support of FAIR-Russia Research Centre. The authors are grateful to A.V.Masalov and N.N. Kolachevsky for the useful discussions and comments.

[1] Dirac P A M *Proc. Roy. Soc. A* **117** 610 (1928)
[2] Dirac P A M *Proc. Roy. Soc. A* **133** 60 (1931)
[3] Anderson C D *Science* **76** 238 (1932)
[4] Anderson C D *Phys. Rev.* **43** 491 (1933)
[5] Schwinger J *Phys. Rev.* **82** 914 (1951)
[6] Baura G et al. *Phys. Lett. B* **368** 251 (1996)
[7] Blanford G et al. *Phys. Rev. Lett.* **80** 3037 (1998)
[8] Antipov U M *Nucl. Phys.* **12** 2 (1970)
[9] Maury S *Hyperfine Interactions* **109** 43 (1997)
[10] http://home.web.cern.ch/about/experiments/atrap
[11] http://home.web.cern.ch/about/experiments/alpha
[12] http://home.web.cern.ch/about/experiments/asacusa
[13] http://home.web.cern.ch/about/experiments/ace
[14] http://home.web.cern.ch/about/experiments/aegis
[15] http://home.web.cern.ch/about/experiments/base
[16] CERN-SPSC-2013-002; SPSC-TDR-002
[17] CERN-SPSC-2011-029/SPSC-P-342 30/09/2011
[18] CERN-SPSC-2009-026; SPSC-P-338
[19] Menshikov L I *Physics-Uspekhi* **178** 673 (2008)
[20] Murphy T J, Surko C M *Phys. Rev. A* **46** 9 (1992)
[21] Surko C M, Greaves R G *Radiation Physics and Chemistry* **68** 419 (2003)
[22] Surko C M, Greaves R G *Physics of Plasmas* **11** 5 (2004)
[23] Amoretti M et al. *Nature* **419** 456 (2002)
[24] Andresen G B et al. (ALPHA Collaboration) *Nature* **468** 673 (2010)
[25] Andresen G B et al. (ALPHA Collaboration) *Nature Phys.* **7** 558 (2011)
[26] Amole C et al. (ALPHA Collaboration) *Nature* **483** 439 (2012)
[27] Gabrielse G et al. (ATRAP Collaboration), *Phys. Rev. Lett.* **108** 113002 (2012)
[28] Hess H F et al. *Phys. Rev. Lett.* **52** 1520 (1984)
[29] Gabrielse G et al. *Phys. Lett. A* **129** 38 (1988)
[30] Glinsky M E, O'Neil T M *Phys. Fluids B* **3** 1279 (1991)
[31] Robicheaux F, Hanson J D *Phys. Rev. A* **69** 010701 (2004)
[32] Hessels E A, Homan D M, Cavagnero M J *Phys. Rev. A* **57** 1668 (1998)
[33] Storry C H *Phys. Rev. Lett.* **93** 263401 (2004)
[34] Speck A et al. *Phys. Lett. B* **597** 257 (2004)
[35] Wesdorp C, Robicheaux F, Noordam L D *Phys. Rev. A* **64** 033414 (2001)
[36] Parkhomchuk V V *Hyperfine Interactions* **44** 315 (1988)
[37] Bluhm R, Kostelecky V A, Russell N *Phys. Rev. Lett.* **82** 11 (1999)
[38] Hansch T W, Zimmermann C *Hyperfine Interactions* **76** 47 (1993)
[39] Campeanu R I, Beu T *Phys. Lett. A* **93** 223 (1983)
[40] Menshikov L I, Landua R *Physics-Uspekhi* **173** 233 (2003)
[41] Widmann E et al. Proposal of FLAIR collaboration, 2005
[42] Heisenberg W *The Physicist's Concept of Nature* **1972** 271 (1973)
[43] Hansch T, Schawlow A *Opt. Commun.* **13** 68 (1975)
[44] Wineland D, Dehmelt H *Bull. Am. Phys. Soc.* **20** 637 (1975)
[45] Wineland D, Drullinger R, Walls F *Phys. Rev. Lett.* **40** 1639 (1978)
[46] Neuhauser W et. al. *Phys. Rev. Lett.* **41** 233 (1978)
[47] Chu S, Phillips W D, Cohen-Tannoudji C *Physics-Uspekhi* **169** 271 (1999)
[48] Phillips W D *Rev. Mod. Phys.* **70** 721 (1998)
[49] Chu S *Rev. Mod. Phys.* **70** 685 (1998)
[50] Cohen-Tannoudji C *Rev. Mod. Phys.* **70** 707 (1998)
[51] Balykin V I *Physics-Uspekhi* **181** 875 (2011)
[52] Balykin V I, Letokhov V S, Minogin V G *Physics-Uspekhi* **147** 117 (1985)
[53] Lett P D et al. *J. Opt. Soc. Am. B* **6** 2084 (1989)

[54] Metcalf H J and P van der Straten *JOSA B* **20** 887 (2003)
[55] Minogin V G, Letokhov V S *Davlenie lazernogo izlycheniya na atomy* (Moscow: Nauka, 1986)
[56] Pavlik B D *Holodnye i ultraholodnye atomy* (Kiev: Naukova Dumka, 1993)
[57] Metcalf H J, P van der Straten *Laser cooling and Trapping* (New York: Springer, 1999)
[58] Letokhov V S, Minogin V G, Pavlik B D *Opt. Comm.* **19** 72 (1976)
[59] Phillips W, Prodan J, Metcalf H Laser Spectroscopy VI (Springer Series in Optical Sciences **40** 162 (1983)
[60] Prodan J V, Phillips W D *Prog. Quant. Electr.* **8** 231 (1984)
[61] Stenholm S Phys. Rep. **43** 151 (1978)
[62] Javanainen J, Stenholm S *Appl. Phys.* **21** 163 (1980)
[63] Letokhov V S, Minogin V G, Pavlik B D *Sov. Phys. JETP* **45** 698 (1977)
[64] Javanainen J *Appl. Phys.* **23** 175 (1980)
[65] Cook R J *Phys. Rev. A* **22** 1078 (1980)
[66] Wineland D J, Itano W M *Phys. Rev. A.* **20** 1521 (1979)
[67] Stenholm S *Rev. Mod. Phys.* **58**, 699 (1986)
[68] Phillips W, Metcalf H *Phys. Rev. Lett.* **48** 596 (1982)
[69] Phillips W D, Metcalf H *Phys. Rev. Lett.* **48** 596 (1982)
[70] Prodan J et al. *Phys. Rev. Lett.* **54** 992 (1985)
[71] Prodan J, Phillips W, Metcalf H *Phys. Rev. Lett.* **49** 1149 (1982)
[72] Phillips W D, Prodan J V, Metcalf H J *Prog. Quant. Electr.* **48** 119 (1984)
[73] Metcalf H, Phillips W D *Comments At. Mol. Phys.* **16** 79 (1985)
[74] Phillips W D, Prodan J, Metcalf H J *Opt. Soc. Am. B* **2** 1751 (1985)
[75] Migdall A et al. *Phys. Rev. Lett.* **54** 2596 (1985)
[76] Lett P D et al. *Phys. Rev. Lett.* **61** 169 (1988)
[77] Dalibard J, Cohen-Tannoudji C *J. Opt .Soc. Am. B* **6** 2023 (1989)
[78] Ungar P J et al. *J. Opt .Soc .Am. B* **6** 2058 (1989)
[79] Dalibard J, Cohen-Tannoudji C *J. Opt. Soc. Am. B* **2** 1707 (1985)
[80] Wineland D J, Dalibard J, Cohen-Tannoudji C *J. Opt. Soc. Am. B* **9** 32 (1992)
[81] Weiss D S et al. *J. Opt. Soc. Am. B* **6** 2072 (1989)
[82] Westbrook C I et al. *Phys. Rev. Lett.* **65** 33 (1990)
[83] Solomon C et al. *Europhys. Lett.* **12** 683 (1990)
[84] Kastberg A et al. *Phys. Rev. Lett.* **74** 1542 (1995)
[85] Aspect A et al. *Phys. Rev. Lett.* **61** 826 (1988)
[86] Kasevich M, Chu S, *Phys. Rev. Lett.* **69** 1741 (1992)
[87] Bardou F et al. *R. Acad. Sci.* **318** 877 (Paris, 1994)
[88] Saubamea B et al. *Phys. Rev. Lett.* **79** 3146 (1997)
[89] Lebedev P *Ann. der Phys.* **6** 433 (1901)
[90] Nichols E F, Hull G F *Phys. Rev.* **13** 307 (1901)
[91] Nichols E F, Hull G F *Phys. Rev.* **17** 26 (1903)
[92] Lebedev P *Ann. der Phys.* **32** 411 (1901)
[93] Minogin V G, Serimaa O T *Opt. Comm.* **30**, 373 (1979)
[94] Letokhov V S *JETP Lett.* **7** 348 (1968)
[95] Letokhov V S, Minogin V G, Pavlik B D *Zh. Eksp. Teor. Fiz.* **72** 1328 (1977)
[96] Ashkin A *Phys. Rev. Lett.* **24** 156 (1970)
[97] Ashkin A *Phys. Rev. Lett.* **25** 1321 (1970)
[98] Ashkin A *Phys. Rev. Lett.* **40** 729 (1978)
[99] Letokhov V S, Minogin V G and Pavlik B D *Sov. Phys. JETP* **45** 698 (1977)
[100] Ashkin A *Opt. Lett.* **9** 454 (1984)
[101] Kazantsev A P *Zh. Eksp. Teor. Fiz.* **63** (1972) 1628; *Sov. Phys. JETP.* **36** 861 (1973)
[102] Kazantsev A P *Zh. Eksp. Teor. Fiz.* **66** 1599 (1974)
[103] Chu S et al. *Phys. Rev. Lett.* **55** 48 (1985)
[104] Letokhov V S, Minogin V G, Pavlik B D *Opt. Commun.* **19** 72 (1976)
[105] Gordon J and Ashkin A *Phys. Rev. A* **21** 1606 (1980)
[106] Dalibard J "Le role des fluctuations dans la dynamique d'un atome couple au champ electromagnetigue", These de doctorat d'etates Sciences Physique (Paris, Universite de Paris, 1986)
[107] Aspect A et al. *Phys. Rev. Lett.* **57** 1688 (1986)
[108] Mollow B R *Phys. Rev.* **188** 1969 (1969)
[109] Lett P D, Gould P L, Phillips W D *Hyperfine Interactions* **44** 335 (1988)
[110] Matveev A et al. *Phys. Rev. Lett.* **110** 230801 (2013)
[111] Weitz M, Schmidt-Kaler F, Hansch T W *Phys. Rev. Lett.* **68** 1120 (1992)
[112] Essen L et al. *Nature* **229** 110 (1971)
[113] Kolachevsky N et al. *Space Sci. Rev.* **148** 267 (2009)
[114] Calmet X, Fritzsch H *Phys. Lett. B* **540** 173 (2002)
[115] Murphy M T, Webb J K, Flambaum V V *Mon. Not. R. Astron. Soc.* **345** 609 (2003)
[116] Kolachevsky N et. al. *Phys. Rev. Lett.* **102** 213002 (2009)
[117] Fischer M et al. *Phys. Rev. Lett.* **92** 230802 (2004)
[118] Huber A et al. *Phys. Rev. Lett.* **80** 468 (1998)
[119] Hansch T W *Physics-Uspekhi* **176** 1368 (2006)
[120] Amole et al. *Nature* **483** 439 (2012)
[121] Kuroda N et al. *Nature Comm* **5** 3089 (2014)
[122] Mohri A, Yamazaki Y *Europhys.Lett.* **63** 207 (2003)
[123] Enomoto Y *Phys. Rev. Lett.* **105** 243401 (2010)
[124] CERN/SPSC 2003-009 SPSC-I-226
[125] Gabrielse G et al, ATRAP Collaboration *Phys. Rev. Lett.* **108** 113002 (2012)
[126] Charman A E, ALPHA Collaboration, *Nat. Comm.* DOI: 10.1038/ncomms2787
[127] Zhmoginov A I et al. *Class. Quantum Grav.* **30** 205014 (2013)
[128] Kellerbauer A et al. *Nucl. Instrum. Meth. Phys. Res. B* **266** 351 (2008)
[129] Testera G et al. *AIP Conf. Proc.* **1037** 5 (2008)
[130] Ferragut R et al. *Can. J. Phys.* **89** 17 (2011)
[131] Nesvizhevsky V V et al. *Nature* **415** 297 (2002)
[132] Voronin A Yu et al. arXiv:1311.7366 [physics.atom-ph]
[133] Amole C et al. *Nat. Comm.* **5** 3955 (2014)
[134] Bressi G et al. *Phys. Rev. A* **83** 052101 (2011)
[135] Stwalley W C and Nosanow L H *Phys. Rev. Lett.* **36** 910 (1976)
[136] Silvera I F and Walraven J T M *Phys. Rev. Lett.* **44** 164 (1980)
[137] Hess H F *Phys. Rev. B* **34** 3476 (1986)
[138] Killian et al. *Phys. Rev. Lett.* **81** 3807 (1998)
[139] Fried Dale G et al. *Phys. Rev. Lett.* **81** 3811 (1998)
[140] Bongs K et al. *Phys. Rev. Lett.* **83** 3577 (1999)
[141] D. E. Pritchard *Phys. Rev. Lett.* **51** 1336 (1983)
[142] Scheid M et al. *Optics Express* **17** 11274 (2009)
[143] Kolbe D et al. *Can. J. Phys.* **89** 25 (2011)
[144] Setija I D et al. *Phys. Rev. Lett.* **70** 2257 (1993)
[145] Lagendijk A, Silvera I F, Verhaar B J *Phys. Rev. B* **33** 626 (1986)
[146] Stoof H T C, Koelman J M V M, Verhaar B J *Phys. Rev. B* **38** 4688 (1988)

[147] Zehnle V, Garreau J C *Phys. Rev. A.* **63** 021402 (2001)
[148] Doyle J M et al. *Phys. Rev. Lett.* **67** 603 (1991)
[149] Mahon R, McIlrath T J, Koopman D W *Appl. Phys. Lett.* **33** 305 (1978)
[150] Cotter D *Opt. Commun.* **31** 397 (1979)
[151] Wallenstein R *Opt. Commun.* **33** 119 (1980)
[152] Phillips W D et al. *Hyperfine Interact.* **76** 265 (1993)
[153] Cabaret L, Delsart C, Blondel C *Opt. Commun.* **61** 116 (1987)
[154] Marangos J P et al. *J. Opt. Soc. Am. B* **7** 1254 (1990)
[155] Batishe S A et al. *Sov. Tech. Phys. Lett.* **3** 473 (1977)
[156] Eikema K S E, Walz J, Hansch T W *Phys. Rev. Lett.* **83** 3828 (1999)
[157] Eikema K S E , Walz J, Hansch T W *Phys. Rev. Lett.* **86** 5679 (2001)
[158] Smith A V, Alford W J *J. Opt. Soc. Am. B* **4** 1765 (1987)
[159] Bjorklund G C *IEEE J. Quantum Elect.* **11** 287 (1975)
[160] Ertmer W, Walls H *Hyperfine Interactions* **44** 319 (1988
[161] Walz J et al. *Nuclear Physics A* **692** 163 (2001)
[162] Pahl A et al. *Laser Physics* **15** 46 (2005)
[163] Kolbe D, Schield M, Walz J, arXiv:1209.1519 [physics.optics] (2012)
[164] Van Roijen R et al. *Phys. Rev. Lett.* **61** 931 (1988)
[165] Hijimans T W et al *J. Opt. Soc. Am. B* **6** 2235 (1989)
[166] Luiten O J et al. *Phys. Rev. Lett.* **70** 5444 (1993)
[167] Donnan P H, Fujiwara M C, Robicheaux F J *J. Phys. B: At. Mol. Opt. Phys.* **46** 025302 (2013); arXiv:1210.6103v1
[168] Kielpinski D *Phys. Rev. A.* **73** 063407 (2006)
[169] Palmer A J, Lam J F *Opt. Soc. Am. B* **3** 719 (1986)
[170] Allegrini M, Arimondo E *Phys. Lett. A* **172** 71 (1993)
[171] Saijun Wu et al., *Phys. Rev. Lett.* **106** 213001 (2011)
[172] Doyle J M et al., *Phys. Rev. A* **52** R2515 (1995)
[173] deCarvalho R et al., *Eur. Phys. J. D* **7** 289 (1999)
[174] Derevianko A *Phys. Rev. A* **64** 011404 (2001)
[175] Cote R et al. *Phys. Rev. Lett* **84** 2806 (2000)
[176] Sinha P K, Ghosh A S *Phys. Rev. A* **72** 052509 (2005)
[177] Perez P et al. *Appl. Surf. Sci.* 255 1 (2008)
[178] Perez P et al. Proposal of GBAR collaboration, CERN-SPSC-2011-029/SPSC-P-342
[179] Mitroy J, Stelbovics A T *J. Phys. B: At. Mol. Opt. Phys.* **27** L79 (1994)
[180] Mitroy J *Phys. Rev. A* **52** 2859 (1995)
[181] Hilico L, Karr J-P, Douillet A, arXiv:1402.1695 [physics.atom-ph]
[182] Diedrich F et al. *Phys. Rev. Lett.* **62** 403 (1989)
[183] Balykin V I *JETP Letters* **40** 251 (1984)